University of Windsor
Scholarship at UWindsor

Electronic Theses and Dissertations | Theses, Dissertations, and Major Papers

11-7-2015

7xxx Aluminum Sheets for Automotive Applications

Sergio Barberis Pinlung
University of Windsor

Follow this and additional works at: https://scholar.uwindsor.ca/etd

Recommended Citation

Barberis Pinlung, Sergio, "7xxx Aluminum Sheets for Automotive Applications" (2015). *Electronic Theses and Dissertations*. 5504.
https://scholar.uwindsor.ca/etd/5504

This online database contains the full-text of PhD dissertations and Masters' theses of University of Windsor students from 1954 forward. These documents are made available for personal study and research purposes only, in accordance with the Canadian Copyright Act and the Creative Commons license—CC BY-NC-ND (Attribution, Non-Commercial, No Derivative Works). Under this license, works must always be attributed to the copyright holder (original author), cannot be used for any commercial purposes, and may not be altered. Any other use would require the permission of the copyright holder. Students may inquire about withdrawing their dissertation and/or thesis from this database. For additional inquiries, please contact the repository administrator via email (scholarship@uwindsor.ca) or by telephone at 519-253-3000ext. 3208.

7xxx Aluminum Sheets for Automotive Applications

By

Sergio Barberis Pinlung

A Thesis
Submitted to the Faculty of Graduate Studies
through the Department of Mechanical, Automotive & Materials Engineering
in Partial Fulfillment of the Requirements for
the Degree of Master of Applied Science
at the University of Windsor

Windsor, Ontario, Canada

2015

© 2015 Sergio Barberis Pinlung

7xxx Aluminum Sheets for Automotive Applications

by

Sergio Barberis Pinlung

APPROVED BY:

_____

R. Carriveau, Outside Program Reader
Department of Civil and Environmental Engineering

_____

J. Sokolowski, Program Reader
Department of Mechanical, Automotive & Materials Engineering

_____

A. Edrisy, Advisor
Department of Mechanical, Automotive & Materials Engineering

August 4, 2015

Declaration of originality

I hereby certify that I am the sole author of this thesis and that no part of this thesis has been published or submitted for publication.

I certify that, to the best of my knowledge, my thesis does not infringe upon anyone's copyright nor violate any proprietary rights and that any ideas, techniques, quotations, or any other material from the work of other people included in my thesis, published or otherwise, are fully acknowledged in accordance with the standard referencing practices. Furthermore, to the extent that I have included copyrighted material that surpasses the bounds of fair dealing within the meaning of the Canada Copyright Act, I certify that I have obtained a written permission from the copyright owner(s) to include such material(s) in my thesis and have included copies of such copyright clearances to my appendix.

I declare that this is a true copy of my thesis, including any final revisions, as approved by my thesis committee and the Graduate Studies office, and that this thesis has not been submitted for a higher degree to any other University or Institution.

Abstract

The automotive industry is interested to reduce vehicles weight, because of the need to reduce the fleet fuel consumption.

Within this scenario, high strength aluminum alloys are a viable alternative to heavier steel currently adopted. In particular 7xxx series aluminum alloys, due to their excellent strength to weight ratio, are drawing the attention of carmakers.

The development of a proper precipitation hardening process is extremely important in order to obtain the best results in terms of strength and it is what has been done in this work for the alloy 7046.

This thesis evaluates the microhardness and tensile testing results. The latter were performed at room temperature, at warm forming temperature and after the alloy was heated up to different temperatures for 5 minutes, at the end of different artificial ageing treatments.

Dedication

To my family, who taught me to remember

“however dark the night, then comes the sun”

Acknowledgements

This project is the result of the double degree program set up between Politecnico di Torino and University of Windsor, with the collaboration of FCA. I will always be grateful to the people involved in its organization for selecting me for this Joint Master Degree project and for giving me the possibility of spending one year of my life in North America. I would like to express my appreciation to the program coordinators of the aforementioned institutions: Dr. Andrzej Sobiesiak, Dr. Giovanni Belingardi, Edoardo Rabino, Mohammed Malik and Ishika Towfic for their irreplaceable role in coordinating this program between two continents.

Special thanks go to my academic advisor at the University of Windsor, Dr. Afsaneh Edrisy who assisted me continuously with her deep knowledge and indicated me the right direction when the route to follow was not clear, with patience and kindness.

I would like to express my gratitude for the assistance given to me by my industrial supervisors: Michele Maria Tedesco and Fabio D'Aiuto from Centro Ricerche Fiat for their guidance and help throughout this year; Jugraj Singh from Chrysler Technical Center for his valuable technical support on this project.

A very important mention goes to the people at the University of Windsor who helped me with the experimental work. In particular, I am profoundly grateful to Dr. Kora Farokhzad, she supported me during the tests with precious advice, bearing my anxiety. Special thanks go also to Mehdi Mehdi and Sharon Lackie, for having helped me with the SEM analysis.

I would like to say "thank you" to the Director of the International Student Center, Mike Houston, and to the Department Secretary and Graduate Secretary, Angela Haskell, for their incomparable help whenever it was needed during this year in Windsor.

I am profoundly thankful to my family for their continuous encouragement and support, not only in the last year. They showed me how the distance can be overcome, being “present” also from thousands of miles away. The first thought goes to my parents, who taught me to work as hard as I can in order to turn my dreams into reality. A huge “thank you” goes to my sisters Alessia and Marta, because I feel so lucky for having them as indisputable reference points. I am deeply grateful to my brothers in law, Francesco and Gabriele, for being more brothers than brothers in law. Of course, very special thanks go to my nephews and nieces: Alberto, Simone, Giorgia and Chiara. They put a smile on my face even in the hardest times, as only children can do.

I am also truly grateful to my other family, composed of my friends. Together, we learned the meaning and the importance of “friendship”, to which we give the value it deserves. Thank you Andrea, Francesca, Francesca, Elia, Valentina and Fabio for always being there for me.

I will never thank enough my second home, Collegio Einaudi, because that is the place where I had the chance to grow up as a person and that gave me the opportunity to meet wonderful people who became irreplaceable friends. In particular, I would like to mention Elisabetta, Lorenzo, Marco, Vincenzo, Isabella and Simone.

I express my gratitude to the fellow adventurers who shared this crazy year with me and with whom I will always have in common a lot of funny memories: Biagio, Ivan, Fabio and Francesco. We know it has not been easy, but it was definitely worth it.

Table of contents

List of tables

List of figures

List of abbreviations

MPGe	Miles per gallon equivalent
SSSS	Super saturated solid solution
VRC	Vacancy rich clusters
GPI	Guinier Preston zone type I
GPII	Guinier Preston zone type I
TTP	Time temperature property
TEM	Transmission electron microscope
SEM	Scanning electron microscope
3DAP	3D Atom probe
RT	Room temperature
UTS	Ultimate tensile strength
HV	Hardness Vickers
EDM	Electric discharge machining
FLC	Forming limit curves
US	United States
FCA	Fiat Chrysler Automobiles
EDS	Energy dispersive X-ray Spectroscopy
SSC	Stress corrosion cracking
DC	Direct chill
PFZ	Precipitates free zones
EAA	European aluminum association
UHS	Ultra high strength

Nomenclature

$t_{aluminum}$	Aluminum thickness
t_{steel}	Steel thickness
E_{steel}	Young's modulus of steel
$E_{aluminum}$	Young's modulus of aluminum
σ_y	Yield strength
σ_o	Resistance of lattice to dislocation motion
k_y	Strengthening coefficient
d	Average grain size
N_v	Total number of vacancies
N	Total number of atomic sites
Q_v	Energy required for the formation of a vacancy
K	Boltzmann's constant
T	Temperature
F	Vickers applied load
l	Arithmetic mean of diagonals of a Vickers indentation
G	Gibbs free energy

1. Introduction

The use of aluminum alloys in automotive applications is expanding. They offer a lightweight alternative to steel, potentially increasing the efficiency of the vehicles. Efficiency gains can be used to lower the amount of energy needed for transportation, reducing the emissions while improving the environmental sustainability [1]. Nowadays, one of the main challenges for the automotive industry is the reduction of the average fleet fuel consumption. The growing concerns on global warming and the greenhouse effect, together with a slight worry about the provision of fossil fuels for the future, pushed indeed many governments to establish strict legislations for vehicles fuel consumption.

The main responsible for the greenhouse effect, and therefore for global warming, is indeed CO_2, whose production is directly related to the type and quantity of fuel burnt. Even though the main sector that produces CO_2 is the industry, precautions and new rules in the automotive segment were needed as well.

New stringent parameters to be met by the vehicles have been introduced in the US in the last few years. In Figure 1.1, as an example, it is shown the trend of fuel efficiency regulations for passenger cars and light duty trucks between 1980 and 2025 in the US. The miles per gallon equivalent (MPGe) is a measure to compare the fuel efficiency of alternative fuel vehicles to that of gasoline driven ones, so that all the different types of propulsions are comparable to each other. For instance the electricity used by electric cars is converted into MPGe through the relationship 33.7 KWh = 1 MPGe [2].

According to the figure, the challenge carmakers have to face is evident, since they have to move the actual fleet average from 33 MPGe up to 54.5 MPGe in 10 years. For the sake of clarity it is better to remind these values refer to vehicles that enter the market in the shown year, and not to those already present on the streets.

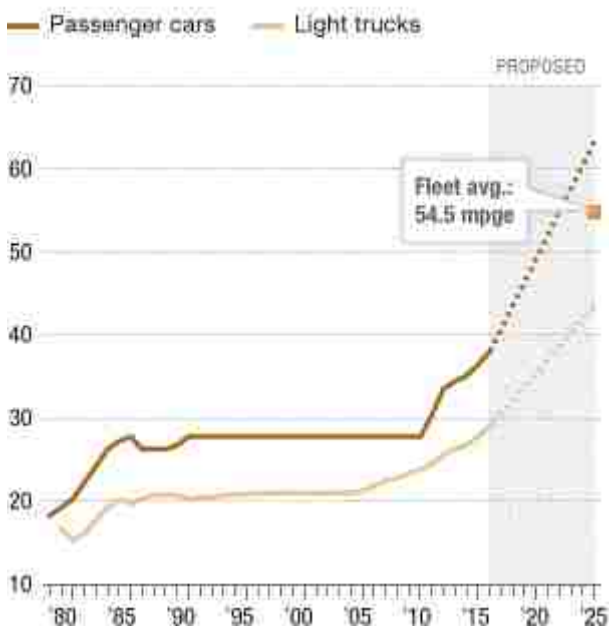

Figure 1.1: Fuel economy standards by model year (in miles per gallon equivalent) **[3]**

One of the most covered ways to lower fuel consumption and improve MPGe figures is the reduction of vehicles weight. According to different studies indeed a 10% mass reduction leads to fuel savings between 1.9% and 3.2% in gasoline engines and between 2.6% and 3.4% in diesel engines; these values refer to non re-sized powertrains. Instead, in the case of re-sizing to match the lower vehicle weight, fuel saving would be more conspicuous that what showed [4].

Weight reduction is usually achieved by designing smaller components or, more frequently, by replacing heavy materials with lighter ones. In this particular context aluminum alloys, together with other light materials such as magnesium and titanium, have been preferred to the heavier steel alloys in some applications.

Currently, for sheet applications in car body engineering AlMg alloys of the 5xxx series or precipitation hardening AlMgSi alloys of the 6xxx series are used. The focus on lightweight brought the attention on high strength AlZnMg(Cu) alloys of the 7xxx series with tensile strength up to more than 600 MPa. The aerospace and sports industry have been benefitting from the utilization of these high strength alloys for decades in terms of significant weight savings and enhanced performance. However, a successful transfer to

the automotive industry requires innovative solutions to allow cost-efficient series production.

According to the tests performed by Aleris [5], replacing a crash component in a car using a 7xxx (not better specified) aluminum alloy instead of boron steel, we obtain very similar crash performance in all the trials saving 40% in terms of mass (thickness increased from 2 to 3.5 mm).

Reported in Table 1.1, a comparison among 5xxx, 6xxx and 7xxx aluminum alloys is shown:

Table 1.1: Comparison of properties of 5xxx, 6xxx and 7xxx aluminum alloys **[6]**

Alloy series	Methods for increasing strength	Yield strength [MPa]	Tensile strength [MPa]
5xxx	Cold working, solid solution	40 - 405	125 - 435
6xxx	Cold working, precipitation hardening	50 - 380	90 - 400
7xxx	Cold working, precipitation hardening	105 - 540	230 - 605

In Figure 1.2, some parts of a car that can be made of aluminum alloys are illustrated:

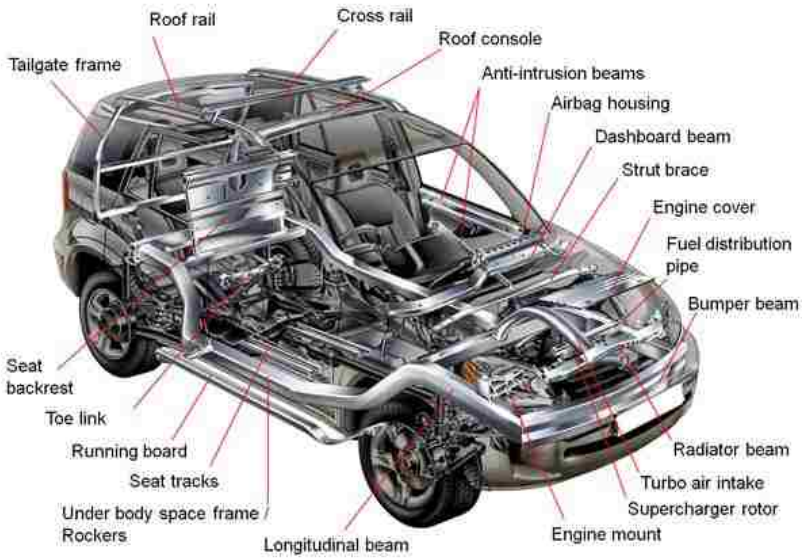

Figure 1.2: Example of the use of aluminum alloys in a car **[7]**

Aluminum alloys are used extensively for such automotive parts as hoods, trunk lids and doors because of their light weight, workability and recyclability. Their market share continues to increase.

The key requirements for automotive closures are panel bending stiffness and dent resistance. The elastic modulus of aluminum (70 GPa) is about one third that of steel (210 GPa). As a result, parts previously designed for steel need to be redesigned to achieve the same stiffness. One way to improve stiffness in aluminum is to increase the ribbing used in the product or increase the part thickness [8]. For closures and body-structure sheets, the thickness should be increased by a factor of about 1.45:

$$\frac{t_{aluminum}}{t_{steel}} = \sqrt[3]{\frac{E_{steel}}{E_{aluminum}}} = 1.44 \qquad (1.1)$$

In which t represents the thickness and E the Young's modulus. The resulting weight saving is about 50%:

$$\frac{mass_{aluminum}}{mass_{steel}} = 1.44 * \frac{density_{aluminum}}{density_{steel}} = 0.5 \qquad (1.2)$$

This thesis, developed in collaboration with the University of Windsor, Politecnico di Torino and FCA (Fiat Chrysler Automobiles), is aimed at studying the 7xxx series aluminum alloysi.e.the AlZnMg(Cu) alloys. They double the yield strength compared to standard 6xxx series automotive alloys. Both alloy families increase their strength significantly by precipitation hardening.

1.1. Thesis organization

The work done is organized in the chapters listed below:

- CHAPTER 2: objectives and procedures. It contains the description of the aims of the thesis with the procedures that have been followed in order to reach them, justifying the adoption of one method instead of another one.
- CHAPTER 3: literature review. In this chapter a theoretical background is given in order to have a better understanding on what happens, step by step, during the precipitation hardening process. The influencing factors are listed and explained and some previous experiments found in literature are described. Moreover, some details concerning warm forming for aluminum alloys are given, as well as a description of the possible fracture surfaces that can be observed after a tensile test is performed.
- CHAPTER 4: methodologies. The section is dedicated to the detailed description of the steps followed during the research and of the material that was used. All the procedures are analyzed: the cutting of the samples, the definition of the heat treatments, the microstructural analysis with the previous preparation of the samples, the hardness and tensile tests (in each condition).
- CHAPTER 5: results and discussion. The data obtained, resulting from the experimental work described in chapter 4, are reported and discussed with the aim of identifying the best precipitation hardening process among the ones tried. Also, the behavior of the alloy during every tensile test is analyzed: at room temperature, again at room temperature but after the material was heated up to different temperatures for 5 minutes and while the alloy is tested at high temperature inside the environmental chamber. Some images concerning the fracture surface of the specimens are reported.
- CHAPTER 6: conclusions. The findings of the research presented throughout the thesis are outlined and summarized. Some recommendations for future work are given.

2. Objectives and procedures

7xxx series aluminum alloys are age hardenable, so their strength can be improved through precipitation hardening. The process and its steps are discussed in the next chapter. Briefly, the material undergoes a heat treatment and small precipitates form inside the microstructure improving the mechanical properties. Two different paths can be followed during the heat treatments: artificial ageing, which is the one used within this work and that gives the highest strength, and natural ageing. Both of them are discussed in the next pages.

The first objective of the thesis is to establish, for the alloy 7046, the precipitation hardening process that gives the optimum mechanical properties i.e combination of high strength and ductility. First of all there is the need to identify a solutionizing process which allows having only one phase in the microstructure, with the formation of a Super Saturated Solid Solution (SSSS) after quenching. Temperature and time are the two parameters that have to be adjusted in order to achieve the wanted condition. Information coming from the literature and an analysis based on the alloy composition (taking into consideration the aluminum-zinc phase diagram) were combined together in order to identify the best possible temperature and time for the solutionizing to occur.

A high quality optical microscope, followed by a more accurate analysis with the scanning electron microscopy (SEM) equipped with energy dispersive spectroscopy(EDS) analysis has been used in order to verify that second phases were not present and that the dissolution occurred properly inside the aluminum matrix. The metallographic sample preparation for the microstructural analysis was performed by cutting, grinding and polishing steps. It was also necessary to identify the proper etchant for revealing microstructure specifically grain boundaries.

Subsequently, three ageing temperatures and seven different time durations were selected, for a total of twenty one different ageing conditions. The Vickers microhardness was measured for each heat treatmen condition. The tensile tests were performed for the conditions that correspond to the highest hardness values.

The tensile tests have been conducted at room temperature, at warm forming temperature and at room temperature after being previously heated for 5 minutes to three different

temperatures. Based on the results obtained from the tensile and hardness tests, the best heat treatments among the ones proposed can be easily identified.

The importance of warm forming for what concerns the stamping of autobody parts is discussed in the next chapter. Good mechanical properties also at high temperatures are required in order to guarantee a good formability.

The last step of the study involves the fracture surface analysis of the specimen after the tensile tests.

3. Literature review

In this section, the precipitation hardening and its steps are described together with the warm forming process for aluminum alloys (especially related to the automotive industry). In addition, some examples coming from the literature are given to highlight the different possibilities in enhancing the mechanical characteristics of 7xxx aluminum alloys. At the end, a description of the possible fracture surfaces that could be present after a tensile test is reported.

3.1 Precipitation hardening

In 7xxx aluminum alloys, Zn is the principal alloying element, but other elements such as copper, magnesium, chromium and zirconium may be specified. Al-Zn-Mg-Cu alloys are usually submitted to different heat treatments to enhance their strength through a process called precipitation hardening or age hardening [9] [10].

They are indeed characterized by a high decrease in solid solubility of alloying elements such as Zn, Mg and Cu with decreasing temperature, meaning the solubility limit of these elements in the Al matrix is much lower at lower temperatures, which is the main requirement for an alloy to be heat treatable [11]. As a matter of fact, if an alloy which does not exhibit this property was submitted to an age hardening heat treatment its mechanical properties wouldn't be affected to a great extent. Another important aspect which has to be taken into account in order to understand if an alloy is heat treatable is the coherency strain in phase boundaries. The necessary condition is the presence of a coherent or semi-coherent boundary. Coherent particles transform to incoherent precipitates as the size increases. The strain energy is reduced and the strengthening effect is weakened. The critical radius for this transition is around 10 nm – 1 μm.

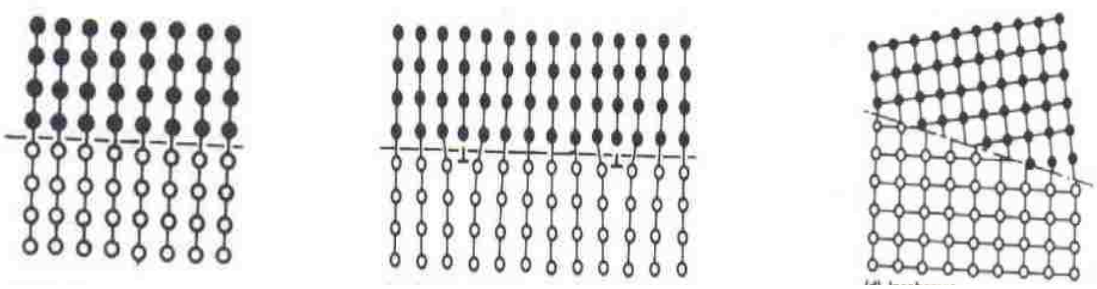

Figure 3.1: From the left to the right: coherent boundary, semi-coherent boundary and incoherent boundary **[12]**

With precipitation hardening small solute rich phases called precipitates are formed throughout the material matrix. They act as an obstacle to dislocations motion, so that a higher energy is required to deform a part, meaning the material is stronger.

It should be reminded here that dislocations are linear crystalline defects of the lattice, involved in the material deformation. More precisely, a component deforms because of dislocations movement, which results in a shift of atoms in the crystalline structure and therefore into an atomic change of shape. Considering the high density of dislocations (10^8 cm/cm^3 in not deformed metals) the overall effect of their simultaneous motion leads to the sample deformation. It is therefore clear how anything hindering dislocations motion results in an increase of the material strength.

The strengthening mechanism deriving from the interaction between precipitates and dislocations is illustrated in Figure 3.2.

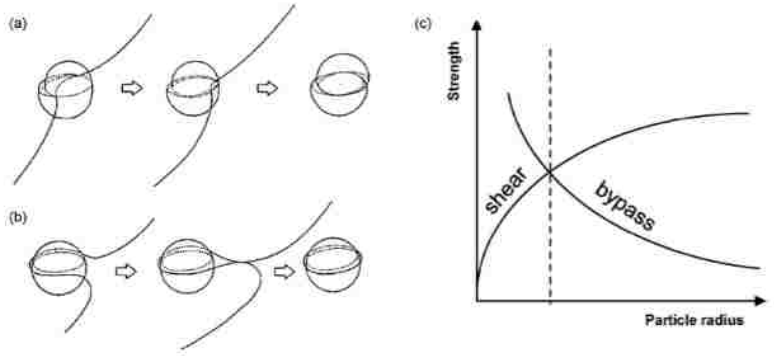

Figure 3.2: Dislocations passing precipitates by shearing (a) or bowing (b). Dependence of the strength from the precipitates radius when sheared or bypassed by a dislocation **[13]**

When dislocations encounter obstacles during their motion they overcome them by shearing (Figure 3.2 (a)) or bypassing (Figure 3.2 (b)) them. As usual, the chosen method is the one that requires the least amount of energy.

The material strength and therefore the required energy associated with each method depends on the radius of the particles to be passed. Below a certain threshold the energy required to shear the precipitate is lower than that required to bypass it; therefore dislocations choose the former way. Above that threshold instead dislocations bypass the precipitate, since shearing would be more expensive.

3.1.1. Sequence of thermal cycles

The sequence of thermal cycles for the heat treatments is the following: solution heat treatment, quenching and ageing.

During solution treatment the material is heated up to a temperature above its solvus line; the temperature line below which β solute rich second phases begin to form into the aluminum matrix α. After a varying holding time the sample is then quenched and brought back into the phase diagram region where β second phases are present again. Finally, in T6 heat treatments the part is held for a varying time at temperatures below the solvus line, otherwise, in T4 heat treatments, it is kept at room temperature (RT). In the former case the ageing process is addressed as artificial ageing and as natural ageing in the latter.

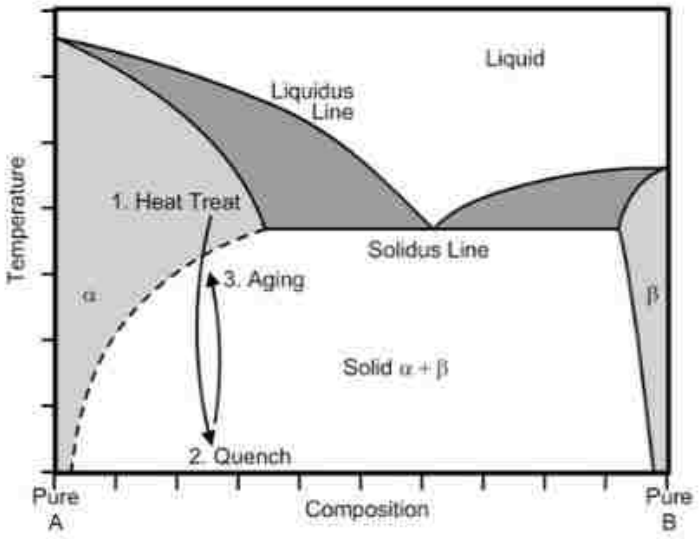

Figure 3.3: Generic phase diagram showing the three different thermal cycles required in precipitation hardening T6 heat treatments **[14]**

In Figure 3.4 we can see the sequence of thermal cycles in a temperature-time diagram:

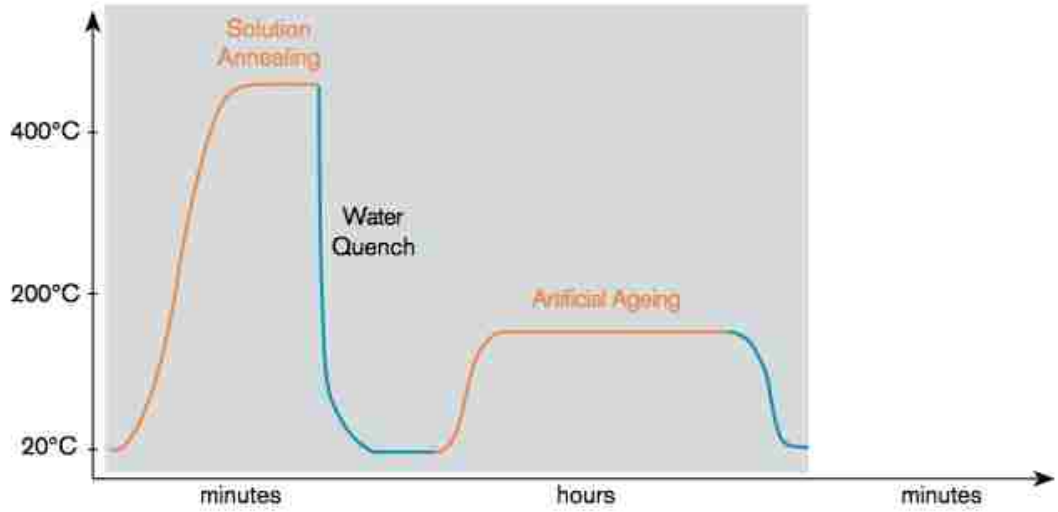

Figure 3.4: Temperature-time diagram for high strength 7xxx series alloys **[15]**

3.1.2. Solution treatment

As previously mentioned, the solution treatment consists in heating the material up to a temperature above its solvus line, in a region of the phase diagram where all the second phases formed during solidification dissolve into the main material matrix, so that solute atoms become available for precipitation hardening.

However, some eutectic phases do not dissolve completely during solution treatment, but their shape is profoundly modified by the thermal cycle. Generally they appear more rounded than before the treatment, thus the strength of the material is increased. It should be pointed out here that sharp and acicular phases, acting as stress concentration sites, increase the chance of crack propagation during deformation, so that failure occurs earlier. Lastly, besides second phase dissolution and modification, the high temperatures adopted in the first step of the T4 or T6 heat treatments enhance the homogenization of solute atoms already dissolved into the aluminum matrix [16] [17]. Indeed, in the as cast condition, solute atoms are not evenly distributed throughout the metal matrix. When submitted to high temperatures instead atoms can diffuse easily and again, since every system tends to the lowest energy condition, they distribute homogeneously in the matrix. This occurs because solute atoms, having different sizes with respect to aluminum atoms, introduce stresses inside the material which are lower when solute atoms are equidistant, meaning they are evenly distributed. Two parameters have to be properly set in the design of a solution treatment process: temperature and time. Time should be selected according to the industrial costs, meaning that beyond a certain period the gain in phase dissolution is so low not to justify a further use of energy. On the other side though, a too short holding time may not be sufficient.

As far as what concerns the temperature, it has a major effect on the dissolution of eutectic phases; high temperatures lead to high atoms mobility and therefore to a better dissolution of second phases, given a constant solutionizing time.

In Figure 3.5 we can see the microstructure evolution of a conventionally cast 7055 alloy related to the different temperatures adopted in the solutionizing step. The amount of eutectic phases at the grain boundaries is drastically reduced with respect to the as cast condition and the higher the solutionizing temperature the lower the

remaining fraction. Moreover those phases still visible present a globular shape, since they underwent a profound transformation.

It is finally worthwhile to observe how the microstructure of this alloy, cast with a conventional technique, does not present globular grains.

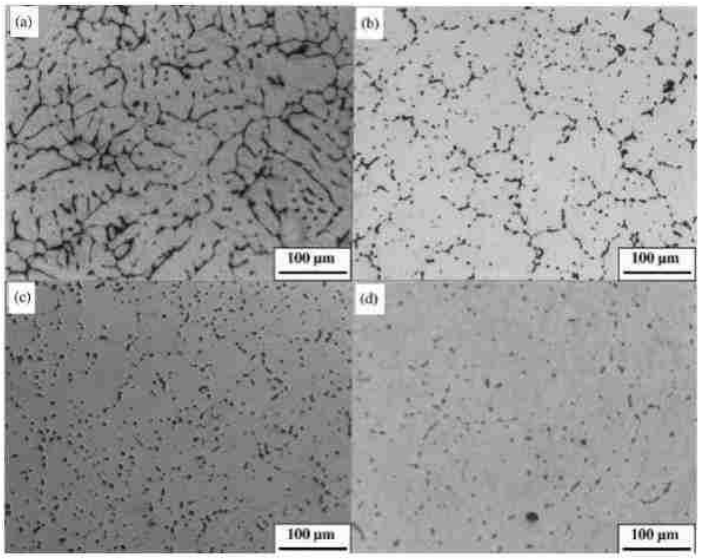

Figure 3.5: Optical micrographs of 7055 aluminum alloy ingots in the as cast condition (a) and after 50 h of solution treatment at 455℃ (b), 470℃ (c) and 475℃ (d) **[18]**

A high dissolution of eutectic phases is desirable, since it increases the saturation level of the metal matrix and therefore its precipitation hardening response; too high solution treatment temperatures should be avoided instead to prevent the phenomenon of incipient melting [19]. This consists in the non-equilibrium melting of the residual phases, meaning that they melt at a temperature lower than the one expected from the phase diagram. This usually occurs when phases characterized by high stability, which would need a long time to be dissolved, are heated up too quickly above their dissolution temperature.

The main drawback of incipient melting is related to the formation of porosities in the subsequent quenching step. In fact, when cooled down the molten metal solidifies but, being surrounded by a solid matrix and not by liquid as during casting solidification, its shrinkage is not compensated by any flow of liquid. Therefore small voids are left in the

matrix. These porosities, diminishing the cross area of the component, increase the stress level, given the same loading conditions, and therefore lead to early failure of the part [19] [20].

Besides material composition, another parameter which deeply affects the incipient melting temperature is the solution treatment heating rate. It is easy to understand how, assuming the microstructure takes a constant time to react to a temperature change, melting is registered at a higher temperature if the material is heated up faster.

An alternative method to improve second phases dissolution and prevent incipient melting at low temperatures is to solutionize a sample in two or three different steps. The same principle of the slow heating rate applies as well; by solution treating a part below incipient melting temperature for a variable amount of time, a lower fraction of second phases is left when the temperature is increased, so that incipient melting occurs at a higher temperature and a higher quantity of solute atoms can be dissolved in the matrix [21] [22].

An additional drawback of high solutionizing temperatures is related to grain growth and recrystallization. In fact, the elongated grains typical of a rolled microstructure become globular and grow during solution treatment [17] [23].

Grain growth should be limited since, according to the Hall-Petch relationship below [24], it leads to a decrease in the material yield strength (the stress at which the component starts deforming).

$$\sigma_y = \sigma_0 + \frac{k_y}{\sqrt{d}} \qquad (3.1)$$

In the Hall-Petch equation σ_y [MPa] is the yield strength, σ_0 [MPa] is the resistance of the lattice to dislocation motion, k_y [MPa*mm$^{1/2}$] is a strengthening coefficient and d [mm] is the average grain size. σ_y, σ_0 and k_y are parameters typical of the material, while d obviously depends on the microstructure.

It is therefore clear how small grains generate an increase in the material strength (the high area of grain boundary prevents dislocation motion) and big grains cause a drop in the yield strength instead.

Summarizing, solution treatment temperature and time should be designed to obtain the maximum dissolution of second phases and to improve solute atoms homogenization in the metal matrix. This eventually results in a higher hardness and strength of the component since more atoms are available for the precipitation stage.

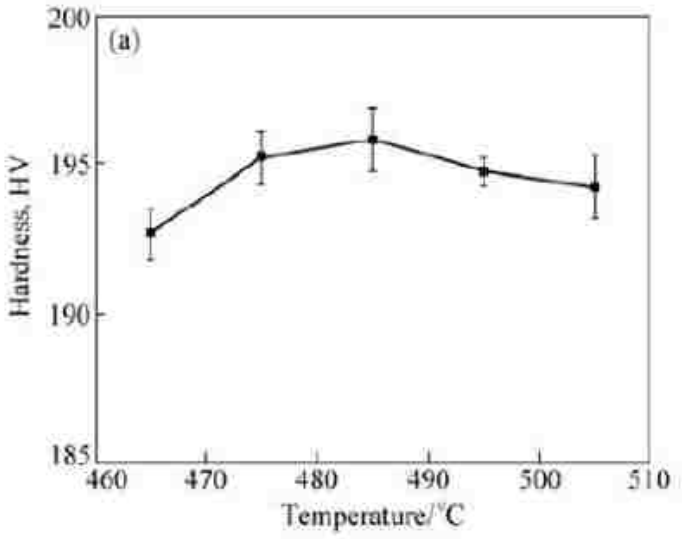

Figure 3.6: Effect of solution treatment temperature on hardness after T6 heat treatment in a 7050 aluminum alloy **[23]**

Attention must be paid not to overtake incipient melting temperature, otherwise a lower fraction of eutectic phases is dissolved and porosities form during quenching, thus worsening material hardness and strength.

However, adopting a slow heating rate or stepped solution treatments the incipient melting point can be increased, so that higher mechanical properties are attainable.

Lastly, the grains size and the level of recrystallization should be monitored to avoid lowering the material yield strength.

3.1.3. Quenching

The second step of T4 and T6 heat treatments is quenching. Here the material in the solution treated condition is cooled down to a temperature where second phases should be present inside the microstructure. According to the phase diagram indeed the solubility of atoms inside the Al matrix decreases with decreasing temperature, so that different compounds are formed.

Nevertheless the aim of quenching is to prevent the formation of these compounds, called quench induced precipitates, and maintain the solution treated condition at room temperature, in order to obtain a Super Saturated Solid Solution (SSSS). In a SSSS the quantity of solute atoms dispersed in the metal matrix is higher than what the solubility limit allows; it is therefore a metastable condition.

The SSSS is a fundamental step for the success of the precipitation hardening process. It is essential indeed to retain as many solute atoms as possible in the metastable condition, so that during the subsequent ageing phase they gather forming small precipitates, which hinder dislocation motion. On the other side, a low level of supersaturation leads to a lower amount of ageing precipitates and therefore to a smaller increase in the material strength, meaning the age hardening response of the material is worse.

To obtain a SSSS the formation of quench induced precipitates should be avoided during quenching. When atoms gather into these compounds they are in fact no longer available for the nucleation of ageing precipitates and the supersaturation level of the Al matrix is decreased, and so does the ageing response of the material [25].

The two variables affecting the formation of quench induced precipitates are atoms diffusion rate and supersaturation level. In aluminum alloys the critical temperature range, where nucleation and growth of these precipitates are maximum, is between 450°C and 200°C [13]. Above this range the supersaturation level is not high enough, while below it the diffusion rate is too low to cause a fast precipitation of second phases.

A properly designed quenching should then ensure that as little time as possible is spent in this critical region; to do so a proper cooling rate has to be selected.

The exact temperature range of the critical region and therefore the cooling rate to be adopted during quenching depends from the quench sensitivity of each material, whose

concept can be better explained by referring to the Time Temperature Property (TTP) diagram shown in Figure 3.7.

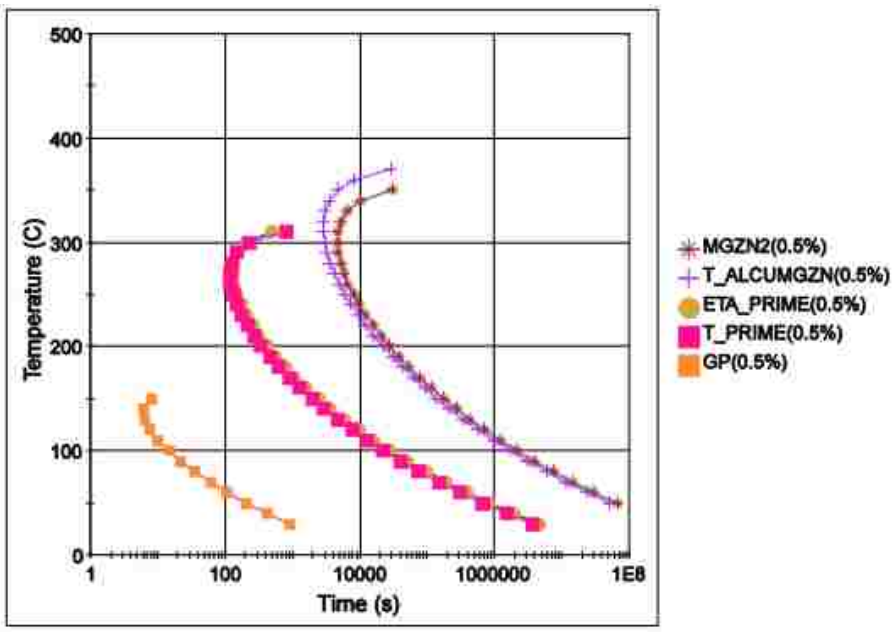

Figure 3.7: TTP curves for 7039 aluminum alloy **[26]**

In a TTP diagram each curve is an iso-property curve, meaning that each point on a single curve is characterized by a strength that is a fixed percentage of the maximum attainable strength of the considered alloy [10]. This percentage is expressed as a function of the time spent at a specific temperature during the quenching stage. In other words the coordinates of each point indicate quenching holding time and holding temperature that lead to the expressed properties. Indeed, as mentioned above, holding a component in a certain temperature range may induce the formation of quench induced precipitates and therefore affects the mechanical properties.

From TTP curves two important quenching parameters can be introduced: the critical temperature range and the transformation time at nose temperature. The former is identified by each curve, given a fixed transformation time, while the latter is the maximum time that can be spent at the nose temperature to get at least 99.5% of the highest properties.

Based on these two parameters the quench sensitivity can be defined for each alloy; the bigger the critical temperature range or the smaller the transformation time at the nose temperature the more quench sensitive an alloy is.

As previously mentioned, the level of supersaturation influences precipitation kinetics during quenching, therefore the higher the amount of solute atoms in Al matrix the higher the chance they gather into quench induced precipitates.

With regards to Zn/Mg ratio it was found instead how a high level of Zn compared to Mg reduces the quench sensitivity. This result is likely to be a consequence of the importance of Mg in the formation of precipitates in 7xxx alloys [27], therefore the lower its relative amount the lower the tendency to form precipitates.

To understand the influence of Cr and Zr it should be reminded that quench induced precipitates usually nucleate at the grain boundaries or on dispersoids and that incoherent interfaces attract atoms more easily than coherent interfaces [10] [28] [29]. Then, being Zr dispersoids finer and coherent with the matrix while Cr dispersoids are coarse and incoherent, the presence of Zr is preferable to Cr from a quench sensitivity perspective [10].

Lastly, the effect of temper on ageing has been verified, but the mechanisms behind the relationship are not clear yet, even though it is likely the implemented cooling rate affects the ageing dynamics and so the mechanical properties [10].

As said before, if the cooling rate is not properly selected and the component is held for long times in the critical temperature range quench induced precipitates will form in the microstructure [29] [30].

Besides the already mentioned effect on the reduction of the supersaturation level, the formation of precipitates during quenching drastically decreases the number of vacancies, which are an essential element for the diffusion of solute atoms during ageing.

Vacancies are point defects of the crystal structure consisting of positions in the material lattice where atoms are not present. Their formation is a function of different factors and their number is expressed by the following formula [31]:

$$N_v = Ne^{-\frac{Q_v}{kT}} \tag{3.2}$$

N_V is the total number of vacancies, *N* is the total number of atomic sites, Q_V is the energy required for the formation of a single vacancy, k is the Boltzmann's constant ($1.38 * 10^{-23} \frac{J}{atom\ k}$) and T is the temperature expressed in Kelvin. During solution treatment the high temperatures reached create vacancies (the higher *T* the higher N_V). As aforementioned, vacancies are a fundamental requirement for atoms motion; these can indeed diffuse inside the lattice only if there are empty sites in their surroundings [31]. Though, when atoms jump from one vacancy to the next one, the vacancy they leave behind is destroyed and therefore can no longer be used for diffusion. It is thus clear how the gathering of atoms in quench induced precipitates reduces solute mobility during the last stage of the heat treatment and therefore the ageing response of the material [32].

The last drawback of quenching precipitation is related to the evolution of the material microstructure during ageing. The presence of already formed coarse and incoherent precipitates indeed deeply affects solute atoms behavior; while they would gather into small and dense precipitates in a properly quenched component, with quench induced precipitates they are attracted by the incoherent interfaces of these. Again this occurs because the energy required to join an already nucleated and big precipitate is lower than forming a new one.

The attraction results thus in the formation of areas where precipitates are absent, known as precipitates free zones (PFZ). In these zones dislocations are free to move without any obstacle, so that the material strength is further decreased with respect to a properly quenched part.

PFZ are located in the surroundings of quench induced precipitates and the coarser the precipitates the wider their extension. Therefore in a slow cooled sample, where quenching precipitates grow bigger and in a higher number, the area fraction of PFZ is higher than in a fast cooled one [33] [34].

In water quenched components the cooling rate is higher than in air quenched ones, therefore in the former case η quench induced precipitates, are smaller and more continuous than in the latter condition. For this reason in the air cooled part wider PFZ evolve during ageing.

Air quenched samples are characterized by lower values of microhardness than those obtained in water quenched ones.

Nevertheless it should be mentioned that a too high cooling rate should be avoided. During cooling indeed a compressive state is introduced in the surface of the component while the interior is submitted to tensile stresses. A high temperature gradient, as results from a very high cooling rate, would increase these residual stresses, which in turn may lead to an early failure of the component [25]; the presence of residual stresses in fact decreases the load a part can withstand before the occurrence of deformation.

Summarizing, during quenching the material is cooled from the solution treatment temperature to obtain a metastable SSSS of solute atoms inside the Al matrix. A high supersaturation level is indeed useful to enhance the mechanical properties during the ageing stage.

To prevent the loss of solute atoms available for the nucleation of ageing precipitates, the formation of quench induced precipitates has to be avoided. It is therefore necessary to select a cooling rate which shortens the time spent in the critical temperature region, where the precipitation rate is higher. Water quenching is usually preferred to air quenching to attain these characteristics.

On the other side though a too fast cooling rate should be avoided as well since it may introduce in the component residual stresses which could result into an early failure.

3.1.4. Ageing

Ageing is the last stage of precipitation hardening heat treatments. If samples are held at room temperature we are dealing with natural ageing. Instead, when components are heated up to a temperature below the solvus line, artificial ageing occurs.

It has already been explained how after quenching the microstructure is in a metastable condition, since the concentration of solute atoms in the Al matrix is higher than what the solubility limit allows. During ageing therefore solute atoms gather into small and dense precipitates which, hindering dislocations motion, increase material hardness and strength.

The driving force leading to the formation of precipitates is once again the need to minimize the energy of the system in the quenched condition. According to what previously mentioned, a high supersaturation level results into a higher density of precipitates. This, from the energy point of view, means that a high concentration of solute generates an increase in the system energy which therefore, to minimize it in the shortest time, forms a high number of precipitates. To understand this concept it should be remembered that during ageing the part is in the region of the phase diagram where second phases should be present, thus destroying the SSSS and nucleating precipitates lowers the overall energy.

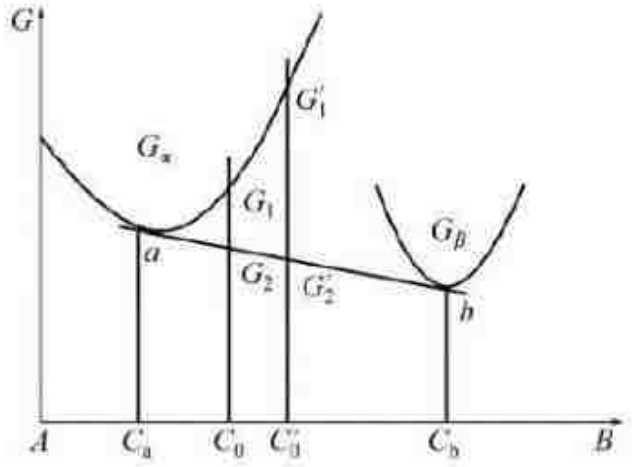

Figure 3.8: Free energy change of precipitation under different supersaturated condition **[23]**

Figure 3.8 illustrates the idea. Given that G_α and G_β represent respectively the Gibbs free energy of the Al matrix α and of the second phase β, by increasing the concentration of solute B from C_0 to C'_0, the matrix energy increases as well from G_1 to G'_1. Then, drawn a straight line between the minimum of the two curves and found the points on this line corresponding to the two different concentrations (G_2 and G'_2), the energy difference $G_1 - G_2$ and $G'_1 - G'_2$ is defined as the precipitation driving force. As it was expected, the driving force is higher with a higher concentration of B since the energy of the matrix is higher as well. In turn, the precipitation driving force is inversely proportional to the

critical radius of nucleation, that is to say, with a high driving force less atoms are required for nucleation. In the end, a small nucleation radius means a shorter time is needed for the formation of a phase, so that a high nucleation rate is obtained and the density of precipitates is increased [23].

After this whole explanation it should be clearer why quenching design is usually addressed to get the highest possible level of supersaturation; there is indeed a direct relationship between solute concentration and density of precipitates.

The main precipitation sequence taking place in Al-Zn-Mg-Cu alloys is the one that follows [28] [30] [34] [35] [36].

$$SSSS \rightarrow GPI \text{ and } GPII \rightarrow \eta' \rightarrow \eta(MgZn_2)$$

From the SSSS, in presence of Vacancy Rich Clusters (VRC), namely patches of the lattice where the density of vacancies is particularly high, Guinier Preston zones of type I (GPI) and type II (GPII) evolve. These are regions of the crystal structure where the concentration of solute atoms is higher. They are the precursors to the metastable η' and stable η.

It should be highlighted that η does not always generate according to the shown sequence. Ageing precipitation is in fact an extremely dynamic process and many factors influence the microstructure evolution, then the above sequence is not strictly followed.

3.1.4.1. Natural ageing

In the presence of available vacancies solute atoms dissolved in the Al matrix start to diffuse to form precipitates as soon as quenching is completed. During natural ageing the sample is held at room temperature, then the diffusion rate is low and long times are required for the formation of second phases. Although, because of the low energy available for atoms diffusion, the precipitation sequence stops at GPI [35], which are therefore responsible of material hardening during natural ageing.

From artificial ageing results it is known that the Zn/Mg ratio of big GPI is equal to 1. This induces to believe in natural ageing the early stages of precipitation are

characterized by the presence of small Mg rich clusters which, evolving into GPI zones and increasing in size, attract Zn atoms until Zn/Mg is 1 [27]. When this condition is reached the precipitation sequence ends and the microstructure is stable.

It was found that early GPI zones show a composition of Cu close to 12 at. %. This value decreases in bigger GPI to 5 at. %, meaning Cu is involved only in the early stages of GPI formation. The presence of Cu inside small GPI is essential since it promotes a higher hardening response of the material in the first precipitation stages [27].

As far as what concerns the morphology of stable GPI zones it is widely accepted they are fully coherent with the Al matrix and feature a spherical shape of alternate Zn and Mg layers [35] [36].

Lastly GPI zones usually form from room temperature up to 140 °C and do not necessarily need the presence of VRC to nucleate [36].

Summarizing, during natural ageing the only precipitate featuring in the microstructure are GPI zones, which in the early stages of their formation are small Mg rich clusters. In the coherent and stable condition they are instead characterized by a spherical shape of alternate Zn and Mg layers (Zn/Mg = 1). Moreover the presence of Cu may enhance the hardening in the early stages of precipitation.

3.1.4.2. Artificial ageing

During artificial ageing the sample is held at higher temperatures with respect to natural ageing, therefore more energy is available for atoms diffusion.

As in natural ageing the first precipitate forming from the SSSS are GPI zones; nevertheless their nucleation occurs in a much lower time. If at room temperature GPI takes almost one day to reach their stable condition, between 121 °C and 130 °C instead they just need 60 min, while their presence is already reported after 15 min only [27] [30].

Through 3D Atom Probe (3DAP) analysis a 3D reconstruction of the precipitates, together with their composition analysis, can be performed. Data about the Zn/Mg ratio of GPI zones are obtained with this technique. It was found that after 30 min at 121 °C the Zn/Mg ratio equals 0.91, indicating that the stable condition has not been reached yet

since Mg is still the dominant element (stable condition at Zn/Mg = 1) [27]. Moreover this datum demonstrates that GPI zones evolve faster in T6 than in T4; after only 30 min at 121 °C indeed their Zn/Mg ratio is higher than after 90 min at RT.

As aforementioned, after 60 min of artificial ageing GPI are stable, therefore Zn/Mg ratio reaches 1. While in natural ageing this condition is the end of the precipitation sequence, in artificial ageing GPI can still evolve into η'. In this case more Zn atoms would be attracted and, starting from their spherical shape, GPI would grow in one direction and would be characterized by an elongated shape and a Zn/Mg ratio of 1.2. Eventually the growth would begin in another direction parallel to the first one and η' would be formed. Alternatively GPI can grow in size and become coarse blocky clusters with Zn/Mg of 1 that would feature in the microstructure even after 24h of ageing [27].

The effect of Cu reported for natural ageing holds in artificial ageing as well. If GPI begin to form from RT, GPII instead nucleate only above 70°C, so that they evolve during artificial ageing only, directly from the SSSS. Differently from GPI, VRC have to be present for their formation, since GPII were found only in samples quenched from solution treatment temperatures higher than 450°C, meaning the amount of vacancies in the matrix is an influential factor [30] [35].

Specific studies on the formation sequence of GPII were not found. The only information in the literature is they are characterized by Zn rich layers organized into a plate like morphology [30].

η' are metastable Zn rich plate like precipitates that are semi coherent with the Al matrix. These compounds evolve from GPI zones but they may nucleate directly from the SSSS attracting solute atoms of dissolving GPI. It should be pointed out indeed that small GPI may grow into stable blocky clusters, evolve into η' or alternatively dissolve [36].

Newly formed η' are characterized by a Zn/Mg ratio of 1.07, while after 24 h of ageing it increases to 1.26. This datum, with those relative to the Zn/Mg ratio of GPI, shows that stable conditions are characterized by a high Zn/Mg, meaning that Zn plays an important role in the stability of the precipitates [27].

η ($MgZn_2$) is a stable and fully incoherent precipitate with a plate like morphology and a size of 15 nm that evolves from η' or directly from the SSSS. Overall η can have 9 different orientations in the crystal structure. The most frequent ones are η_1, η_2 and η_4, to

which different evolution paths are associated; η_1 nucleates directly from the SSSS, η_4 grows on defects such as grain boundaries and dislocations while η_2 evolves from η'. This transformation occurs gradually and consists in η' attracting Zn atoms and slowly changing their shape [36].

Briefly summarizing the precipitation sequence taking place during artificial ageing, in the early stages small GPI zones with a Zn/Mg of 0.91 nucleate. These can grow in size reaching a stable condition with Zn/Mg of 1, grow and evolve into η' or dissolve. The metastable and semi coherent precipitate η' begins to form after 60 min of ageing at 121 °C and stabilizes after 24h with a Zn/Mg of 1.26. It can evolve from GPI or directly from the SSSS. At longer ageing times Zn atoms join η' which further transforms into the stable and incoherent $MgZn_2$ η. This precipitate can alternatively nucleate on lattice defects or from the SSSS.

GPI and η' are the hardening precipitates, while η growth should be avoided since it causes a drop in the material strength [36]. In the first stages of ageing the precipitates present inside the matrix (GPI and η') are characterized by a relatively small radius, therefore they are sheared by dislocations, so that the material strength increases. η instead are beyond the threshold radius and are bypassed by dislocations, leading to lower properties.

It is thus usually desirable to stop the ageing treatment at the peak strength before η nucleates and the strength decreases, in which case ageing would be addressed as overageing. To avoid overaged conditions the selection of ageing time is therefore crucial. Nonetheless the main parameter to be monitored is the ageing temperature. Increasing ageing temperature the peak strength is reached in a shorter time since the diffusion rate of atoms increases, but the obtained value is lower than what results from lower temperatures ageing.

It is thus now better clear how ageing temperature and time should be appropriately chosen in order to obtain the desired mechanical properties.

3.1.5. Examples of precipitation hardening process control

Age hardening of aluminum alloys has been investigated in the past years. Many researches were concentrated on the precipitation and on the related hardening of the alloy both from the experimental and theoretical point of view.

For the purpose of the alloy design, understanding the relationship between fracture behavior and microstructure is a vital requirement. Fracture behavior of Al-alloys is essentially controlled by the volume fractions and character of inclusions, dispersoids and precipitates. The micromechanisms governing fracture characteristics of age hardened alloys depend on coherency and distribution of precipitates, grain size and shape, grain boundary precipitates, the presence of other particles which results from impurities.

The yield stress and the ductility are known to be paradoxical: the maximum of age hardening corresponds to the minimum of ductility. The study conducted by Chemingui et al. [37] checked the heat treatment that offers a better compromise: after achieving a high yield strength, heat treatments can give rise also to an increase in ductility. The chemical composition of the alloy studied is shown in Table 3.1:

Table 3.1: Chemical composition of the investigated material (wt %) **[37]**

Al	Zn	Mg	Cu	Mn	Fe	Si	Ti	Cr
Balance	4.6	1.2	0.065	0.3	0.25	0.23	0.036	0.18

After solution treating of the alloy specimens at 475ºC for 24 hours and icy water quenching, different ageing treatments were performed. Such preparation of the samples allowed the observation of the evolution of the microstructure, so the precipitation process and the study of the mechanical properties by means of indentation and tensile tests.

The main experimental results and conclusions were:

- After various states of ageing, the alloy showed significant changes in the microstructure and mechanical behavior. After quenching, the microstructure was characterized by a high ductility, whereas the aged sample at 135ºC,

corresponding to the maximum value of hardness, revealed the presence of small η' precipitates.

- The yield strength monotonously varies with the hardness. The ratio between them was found almost constant (about 2.2) for all the investigated samples. On the other hand, the strain hardening exponent, the difference between the tensile strength and yield strength and the elongation vary proportionally with the plastic zone dimensions.
- Whatever the treatment, the samples rupture is considered in a ductile mode.
- After two-step ageing treatment, the specimen shows a fine distribution of η' precipitate. The two steps aged samples have a higher value of yield strength and the alloy retains its ductility.

Another study which has been considered and from which the heat treatment proposed in this thesis has been taken as a reference is the one carried out by Sevik et al. [38]. Their work was focused on the effect of precipitation hardening treatment on the surface roughness and mechanical properties. The mechanical properties of the specimens were estimated by hardness and tensile tests. Additionally, the ductility properties and fracture behavior of the specimens, fractured in the tensile tests, were analyzed with a scanning electron microscopy (SEM) of their fracture surfaces.

Table 3.2: Aging parameters of the material used in the experiments **[38]**

Material	Solutionizing	Quenching	Artificial ageing [ºC]	Ageing time [h]
AA7075	480ºC / 2h	Icy water	120 155 185	1 4 10 14 24

The highest hardness of 210 HV was obtained with ageing treatment at 155 ºC for 14 hours. These values of hardness are so high since the 7075 alloy is one of the strongest among the 7xxx series. The European Aluminum Association (EAA) classified alloys with yield strength greater than 300 MPa as high-strength, while those exceeding 400

MPa are rated as ultra-high strength. Heat treatable 7xxx alloys are the only ones in this category.

3.2. Warm forming

Vehicle weight reduction can be accomplished by a combination of redesign and increased use of lightweight materials, such as aluminum alloys. However, a number of technical problems must be overcome before aluminum alloys can replace conventional mild steel for many applications. Among these problems is the reduced formability of aluminum autobody alloys compared to steel.

In order to assess the potential for improving the ductility of aluminum autobody alloys at elevated temperatures, an actual forming operation was carried out on heated production dies [39].

Studies carried out by Morris and George tried to eliminate the heat treatment of the formed part in order to reduce the cost of high strength aluminum stampings. Usually, the followed method of manufacturing a high strength aluminum part is to form an annealed age hardenable alloy, followed by solution heat treating, and then artificial aging. The consequence of this process is a long time cycle, additional handling and heat treating facilities. The extra cost of heat treating represents, therefore, a significant portion of the total cost of the part. Because of the aforementioned reasons, it has been developed a process to warm form parts directly from previously work hardened or age hardened aluminum sheet. In order to reach this objective, it is necessary to form at a temperature high enough to give adequate formability but low enough to preclude substantial strength loss due to recrystallization or overaging [40].

Taylor et al and Ayres have shown that the tensile elongation of annealed Al-Mg alloys could be increased by testing at elevated temperatures, if the strain rates were low [41].

In Figure 3.9 we can see the curves showing the change in room temperature yield strength, after holding the materials for 5 minutes at different temperatures.

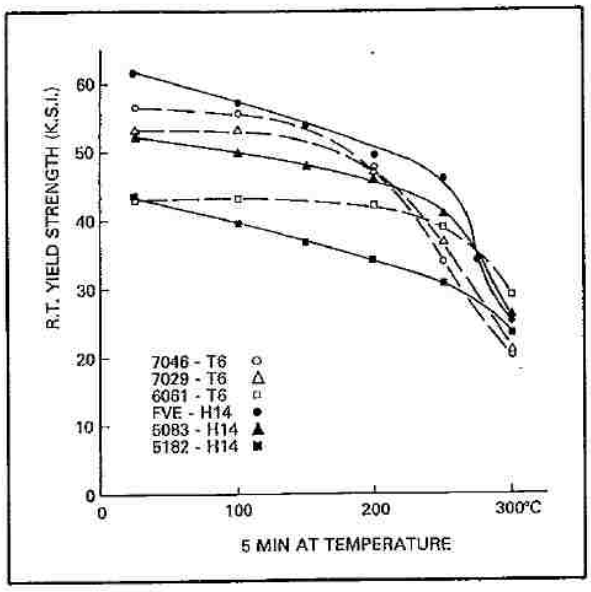

Figure 3.9: Recovery curves showing room temperature yield strengths after 5 minutes at the temperatures indicated **[40]**.

At some temperature, the work hardened alloys recrystallize and the age hardened alloys overage. The temperature at which a rapid decline in strength begins define the maximum, and usually optimum, forming temperature. In the example given in the previous image, 5 minutes at temperature was used since it corresponds to the maximum time expected in a production trial. As can be easily imagined, shorter times spent at a certain temperature will increase the maximum forming temperature.

From what has been seen in an elevated temperature load-elongation curve, work hardening (as defined by the strain to maximum load) is negligible and deformation continues at approximately a constant true stress, up to plastic instability and fracture. The tensile elongation decreases while increasing strain rate.

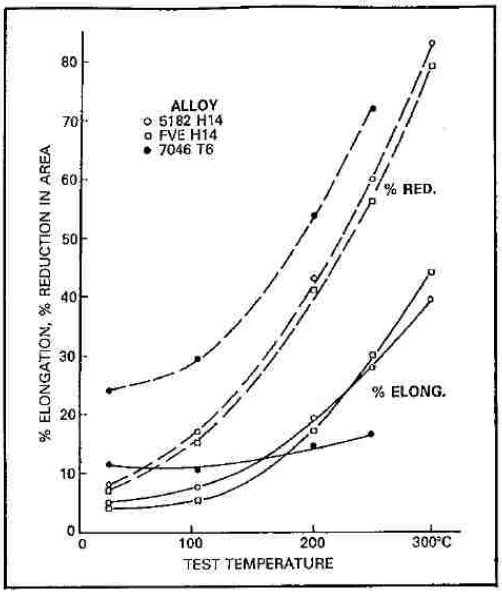

Figure 3.10: Variation in tensile elongation and reduction in area at fracture with test temperature at a strain rate of 10/min **[40]**.

Strain rate hardening is an important property of high strength aluminum alloys during warm forming since the work hardening is small and thus only strain rate hardening, which control diffuse necking, prevents plastic strain from concentrating in a localized neck. At elevated temperature and low strain rate the high elongation of Al-Mg alloys is due to their high strain rate sensitivity while the low elongation of the age hardened alloys is due to their lower strain rate sensitivity.

Another factor that will tend to reduce the tensile elongation at high strain rates is the heating of the sample during deformation. As the specimen is deformed, a diffuse neck develops and the heat generated in the specimen will be greatest in the center of that part, where the strain is the highest. The increase in temperature will produce a gradient in the strength of the material which will tend to concentrate the strain and lead to localized necking. At high strain rates the effect becomes more pronounced because the flow stress is higher and the heat generated cannot be dissipated immediately. This “adiabatic” heating will be of more importance in warm forming than in cold forming because the flow stress varies more with temperature and because the materials are closer to the point of structural instability.

For the age hardened alloys tested by Morris and George [40], among which there is also the one investigated in this thesis (7046), the optimum forming temperature is about 200 Celsius degrees. At this temperature these alloys will have a good behavior for what concerns enhanced bending or drawing but, because of the low strain rate hardening, they would not be expected to perform well during stretch forming.

In order to verify the manufacturing feasibility of the warm forming process several trials were held on production tools. The type of parts selected were thick structural parts requiring high strength and represented a variety of stretch-draw forming conditions. Forming trials were held on a bumper reinforcement, bumper facebar, bumper absorber center mounting bracket and bumper guard.

Since the formability decreases rapidly with decreasing temperature, cooling of blanks in the die is important. A method found to reduce the rate of cooling was to employ a resin base isolative lubricant. A concern was related to the need of heating the dies or not. The warm aluminum blank will rapidly lose heat when in direct contact with cold dies, this factor can have significant influence. With a slow hydraulic press, for example, the blank could lose enough heat to create forming problems by bringing the aluminum below the formable temperature. In order to make parts, these blanks had to be heated more than normally required to compensate for heat losses. In another case, when a mechanical press operating at high volume production speed was used, the parts were formed before substantial heat loss occurred. In a production run of warm forming the dies would absorb heat and reduce the heat loss effect.

3.2.1. Industrial applications

More recent studies [42] regarding the stamping of autobody parts have shown that the use of heated dies complicates the process and increases the costs. Present R&D efforts are focused on heating the sheet to warm forming temperature while keeping the dies at room temperature. Researchers hope to establish a practical and robust process that increases the formability of aluminum sheet for forming more complex parts with difficult geometries.

Other researches focused on warm forming were conducted for 7xxx aluminum series [15], according to which warm forming at temperature levels far below those for press hardening steel helps to overcome the moderate formability of 7xxx alloys at room temperature. AMAG developed a Cu-containing alloy called AMAG TopForm UHS for replacing press hardened steel in automotive components like B-pillars or side impact beams. It is an AA7075 type alloy optimized for warm forming in the long-term stable T6 peak age delivery temper, it shows excellent warm forming behavior at temperatures between 170 and 230 ºC.

Figure 3.11: Side impact protection made from AMAG TopForm UHS **[15]**.

While warm forming at 170ºC with just one or two minutes process time has almost no impact on strength, a slight increase to 200ºC reduces the strength by some 50 MPa.

AMAG TopForm UHS doubles the strength compared to a standard AA6016 alloy. A high specific resistance to denting and high specific crash performance make this alloy ideal for the replacement of press hardened steels (side impact protections or bumper beams).

While time consuming process steps at high temperatures like solution annealing and artificial ageing are done in the rolling mill in an efficient and controlled manner, it just takes seconds in the press shop to heat up the blank to a temperature of around 200ºC. There is no requirement of rapid quenching after warm forming. A reliable and stable heat treatment process at the rolling mill provides long-term stable mechanical delivery properties in T6 temper and offers stable high level properties after press and paint shop

within a robust process window. New innovative thermal joining technologies recently introduced to the automotive industry have been successfully tested for this AMAG high strength alloy. Moreover, mechanical methods and hybrid joining in conjunction with adhesive bonding extend the joining portfolio.

3.3. 7xxx series alloy optimization

The desire to achieve high levels of fracture toughness and stress corrosion cracking resistance simultaneously with high strength in 7xxx series aluminum alloys has been the subject of attention over the years [43]. Such alloys are used in high integrity structural applications such as aerospace components, where careful control of both chemical composition and processing conditions is applied in order to deliver the necessary levels of performance. The development of similar alloys for use in high pressure gas cylinders has been described as being significant to the aluminum industry, and requires a particularly demanding combination of strength, toughness and corrosion cracking resistance. The aim of the study conducted by Clinch et al [44] was to control composition, processing and microstructure in order to maximize strength whilst maintaining adequate fracture toughness. The importance of factors such as the size and distribution of coarse intermetallic particles, quench rates recrystallization and grain structure are well known for 7xxx series alloys.

The strength of this kind of alloys depends principally upon its compositional detail [45], since the precipitate phases promote the greatest strength contribution and these depend upon the Zn/Mg ratios and copper content. In general, fracture toughness is at its highest in the underaged condition, passes through a minimum at peak strength then recovers again during overaging [43] [46].

A. Mukhopdhyay [47] introduced fundamental basis of high strength wrought Al-Zn-Mg and Al-Zn-Mg-Cu alloy system design and processing parameters. Major alloying element must have adequate solid solubility in the aluminum matrix, it encourages the nucleation of precipitates formed in the constituent binary system or induces the nucleation of fresh binary/ternary precipitates. Commercial Al alloys may further contain

a third major element that either accelerates the precipitation process and/or forms fresh binary/ternary/quaternary phase precipitates. Minor alloying elements like Cr, Mn and Zr form compounds with Al and other alloying elements, inhibiting grain growth and recrystallization (Sc). Sc together with Zr is a good grain refiner. Small additions of either Sc (0.23 wt%) or Ag (0.35 wt%) greatly improve the SCC resistance. As a drawback that limits its usage, Sc is an expensive addition. 7xxx aluminum alloys contain:

- 3.5 - 8.7% Zn
- 1.0 - 3.1% Mg
- Up to 2.6% Cu
- Up to 0.28% Cr
- Some other elements like Zr, Ti, Mn, (impurities of Fe and Si)

A combination of unrecrystallized grain structure, the presence of a uniform distribution of $Al_3Sc_XZr_{1-X}$ dispersoids and smaller grains and narrow Precipitates Free Zone (PFZs) adjacent to the grain boundary are responsible for improved stress corrosion cracking (SCC) resistance of the Sc-bearing alloy.

I. Polmear and M. Couper stated that the aged Al alloys have the highest specific strength of all commercially available alloys at temperatures up to 100^0C [48]. Above this temperature, mechanical properties decline rapidly due to coarsening of fine precipitates responsible for alloy strength.

S. Senkova et al. [49] [50] evaluated the effect of combined addition of Sc and Zr on microstructure and mechanical properties of the direct chill (DC) cast ingots of developmental Al-Zn-Mg-Cu alloys subjected to homogenization, solution treatment and aging that show superior properties of any commercial cast alloy. Sc containing alloy exhibited similar properties to wrought 7075-T6 alloy.

During the EAA (European Aluminum Association) 2011 conference, the effect of chemical composition on the microstructure, mechanical properties and susceptibility to hot tearing of Al-Zn-Mg-Cu cast alloys were tackled by two teams: H. Zak and Tonn as well as S. Bozorgi, M. Justl and P. Schumacher [51] [52]. It was found that Mg and Zn

make the highest contribution to yield and tensile strength. Cu content above 2.9 wt% has a deleterious effect on mechanical properties forming brittle grain boundary particles which cannot be dissolved completely during solution treatment for 16 hours at 470°C.

3.4. Fracture surface analysis

Fractographic observation and fractography has been a powerful tool used for the determination of failure causes in materials or components. A scanning electron microscope is generally used because it provides a practical range of magnifications suitable for the investigation.

Type of fracture can be roughly divided into two categories, which are brittle and ductile fractures. During brittle fracture a little amount of plastic deformation can be detected, what happens is a sudden failure without warning. Ductile failure, on the contrary, exhibits rough and dull fracture surfaces with gross plastic deformation, therefore allowing more time to correct or prevent such failures [53].

Brittle materials normally exhibit flat fracture surfaces consisting of transgranular cleavage facets. This type of fracture give small areas of fracture surface; hence, requiring low specific surface energy to produce two new fresh fracture surfaces. Therefore, the fracture energy is low in this case. When the crack is initiated possibly at the inclusion, the metal grains then readily cleave along the low fracture energy crystallographic plane. The stress lines are steps between cleavage or parallel planes, which are always convergent in the direction of local crack propagation. Transgranular cleavage fracture is usually associated with defects such as cracks, porosities, inclusions or second phase particles in which dislocations movement is obstructed. The stress is therefore concentrated in front of these defects, initiating a crack of a critical size. The propagation of this crack then finally causes the global failure with very little plastic deformation.

Considering a tensile sample that underwent a ductile fracture, it is possible to see necking occurring along the specimen gauge length. Within the necking area, microvoids

are formed probably around the particles. During the time of the test, these microvoids expand and join together to create a crack with its plane perpendicular to the axis of the tensile force applied. Ductile materials show a considerable amount of plastic deformation before fracture, providing rough fracture surfaces with relatively high surface areas. Ductile fracture therefore requires higher energy to create two new fresh fracture surfaces in comparison to the energy required to cleave flat brittle surfaces. With the help of a SEM, it is evident how a ductile fracture surface consists of ductile dimples or microvoids.

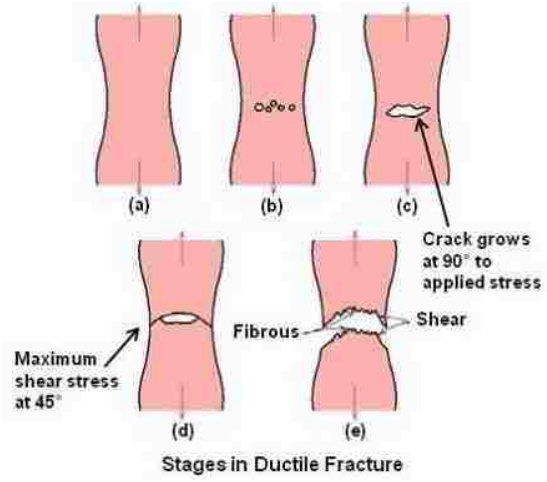

Figure 3.12: Schematic drawing of the subsequent stages in ductile fracture **[53]**

During loading, inclusions or second phase particles (that act as microvoid initiation sites) lose coherency with the matrix, forming a microvoid around each particle. After a while, the expansion of microvoids leads to their coalescence, giving the complete failure.

Now, an example regarding fracture surface analysis for aluminum alloy is given, taken from the study conducted by Sevim et al. [38] on 6xxx and 7xxx series.

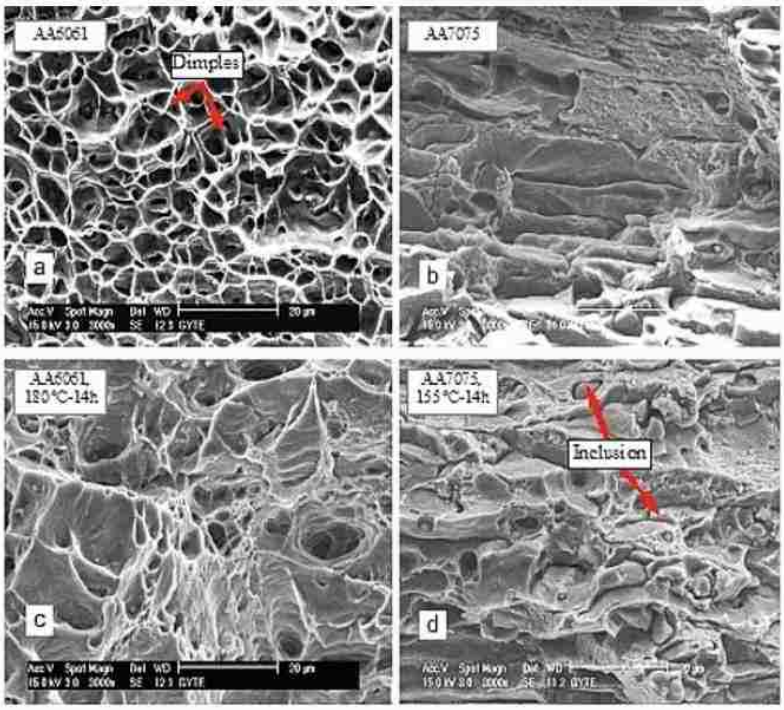

Figure 3.13: SEM images of the fractured specimen surfaces **[38]**

Figure 3.13 shows SEM images of the fractured surface taken from fractured tensile test specimen. The alloy 6061 exhibits ductile fracture. The dimples and network structures were determined to be dominant in the images. The images coming from aged specimens have a smaller number of ductile dimples. In the case of alloy 7075, brittle fracture occurred and cleavage facets are visible.

4. Methodologies

In this chapter the composition of the alloy investigated and the procedures followed in the experimental work are presented and explained.

4.1. Alloy composition and samples cutting

The aluminum alloy studied in this thesis is a 7xxx series provided by FCA (Fiat Chrysler Automobiles), which is the industrial partner of the work. More specifically, the alloy is the 7046, with the composition here reported (wt%):

- Zn - between 6.3 and 6.6%
- Mg – between 1.4 and 1.6%
- Cu – between 0.1 and 0.2%
- Zr – between 0.1 and 0.15%
- Fe – max 0.2%
- Si – max 0.1%
- Mn – max 0.05%
- Cr – max 0.05%
- Ti – max 0.05%

The samples were cut starting from square sheets, 300 mm x 300 mm, whose thickness was 1.25 mm. A wire-cut EDM (Electric Discharge Machining) machine was used for cutting the samples for the tensile tests. This cutting method allows obtaining a desired shape using electrical discharges. Material is removed from the workpiece by a series of rapidly recurring current discharges between two electrodes, separated by a dielectric liquid and subject to an electric voltage. In wire electrical discharge machining (used for the research), a thin single-strand metal wire, usually brass, is fed through the workpiece, submerged in a tank of dielectric fluid, typically deionized water. The advantages of using an EDM machine are basically two: the material does not undergo a too high thermal stress and the cut surface is extremely smooth, so it avoids the formation of

rough zones in which the stress would be concentrated during the tensile test falsifying in this way the result, which would not be significant.

Other coupons (1 inch x 1 inch) were cut for the hardness measurements and microstructural analysis.

The EDM machine, during its operation, followed a file on which a drawing prepared with the software Solidworks was saved. The standard followed for the drawing is the ASTM E8 for sheet-type standard specimen:

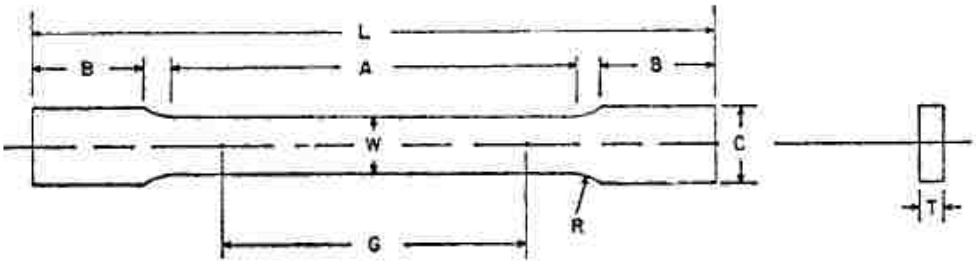

Figure 4.1: Sketch of the specimen that follows the ASTM E8 standard **[54]**

Table 4.1: Dimensions for standard specimens given by ASTM E8, sheet-type specimens **[54]**

	Dimensions [mm]
G - Gage length	50 ± 0.1
W - Width	12.5 ± 0.2
T - Thickness	thickness of material
R - Radius of fillet, min	12.5
L - Overall length, min	200
A - Length of reduced section, min	57
B - Length of grip section, min	50
C - Width of grip section, approximate	20

In Figure 4.2 and Figure 4.3 we can see the aluminum sheets as they were received, the specimens for the tensile tests (fractured after the experiments) and the EDM machine, also with an aluminum sheet in place just before being cut.

Figure 4.2: On the left, the aluminum sheets as received. On the right, the specimens cut with the EDM machine after having tested them.

Figure 4.3 On the left, the EDM machine used for cutting the specimens. On the right, the aluminum sheet placed in the machine before being cut.

4.2. Heat treatment utilized

The first step in the precipitation hardening process is, as already discussed, the solution heat treatment. In defining the temperature and time more adequate for the studied alloy, two things have been considered: the alloy composition, looking at the aluminum-zinc phase diagram, and previous studies found in literature. After some trials, the solutioning temperature selected was 480ºC and the solutionizing time 2 hours. The whole heat treatment procedure established (already reported in chapter 3) is summarized in table 4.2.

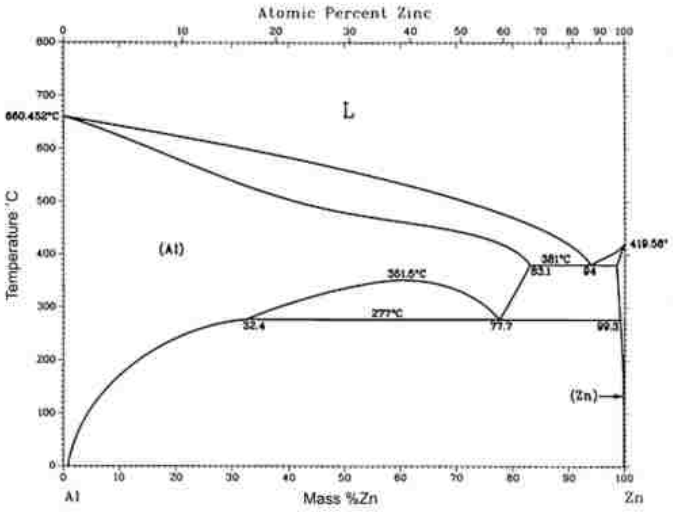

Figure 4.4: Aluminum – Zinc phase diagram **[55]**

Table 4.2: Heat treatment procedures followed in the research

Material	Solutionizing	Quenching	Artificial ageing [ºC]	Ageing time [h]
AA7046	480ºC / 2h	Icy water	120 155 185	1 4 10 14 17 20 24

The specimens and the coupons, in the furnace for 2 hours, are then rapidly quenched in icy water in order to avoid the formation of quench induced precipitates that would interfere with the proper precipitation process which occurs during ageing.

3 different ageing temperatures and 7 ageing times were chosen. All the possible combinations were tested for what concerns the hardness measurements, while only the best conditions according to the hardness results were tested with the tensile machine. The tensile tests are carried out at room temperature, at warm forming temperature and at room temperature after the alloy has been heated up to a certain temperature for 5 minutes, as it will be better explained in the next pages.

In Figure 4.5 we can see the furnace that has been used for the solutionizing treatments but also for artificial ageing, with the controller on the left through which the desired temperature can be set.

Figure 4.5: Furnace used for the solutionizing and ageing phases

4.3. Microstructural analysis

4.3.1. Samples and surface preparation

In order to verify the effectiveness of the solutionizing process, a microstructural analysis was carried out to exclude the presence of second phases. The sample mounting and preparation needed for the observation with the optical microscope and the SEM was done following a procedure that involved the usage of different machines, in the laboratories of the University of Windsor.

First of all, the solutionized coupon was further cut using the cutting machine reported in the figure below, in order to reach a size that would fit in the mounting cylinders. These small cylinders, open on one side, are then filled with the mounting resin after the material that has to be analyzed is placed in the middle of the base. The resin, which at first is liquid, solidifies in 20 minutes.

The cutting machine here shown works thanks a rotating blade with adjustable rotation speed. The blade needs to be cooled down in order to avoid overheating.

Figure 4.6: Cutting machine used for the preparation of the samples for the microstructural analysis

After the sample was mounted, grinding and polishing followed in the preparation process. Both of them have been done with the polishing machine, onto which sand paper or polishing cloths can be positioned on the rotating plates depending on what it is needed:

Figure 4.7: Polishing machine used for grinding and polishing

During grinding, sand paper was used, employing step after step a finer size of the abrasive surface. After that, the usage of a polishing cloth with alumina was necessary in order to get rid of all the scratches on the surface of the sample. The polishing process requires time, until all the scratches on the surface of the sample are eliminated, which is an essential requirement for the observation with microscopes (both optical and SEM).
In Figure 4.8, we can see how the mounted sample looks like, ready to be etched and observed with the optical microscope.

Figure 4.8: Mounted sample ready for microstructural observation

After the surface is ready, the right etchant has to be used in order to reveal the microstructure with its grain boundaries. Each material requires the usage of a proper etching solution which can react with the surface of the sample to be analyzed. Not only the etchant has to be identified, but also the time of exposure needs to be properly set. Different etchants have been prepared and tried, but the one that worked better for this specific alloy was the Kellers etchant, whose composition is reported in Table 4.3:

Table 4.3: Amount of each constituent in the Kellers etchant **[56]**

Distilled water	190 ml
Nitric acid	5 ml
Hydrochloric acid	3 ml
Hydrofluoric acid	2 ml

In the case of the alloy 7046, the time of immersion in the etchant needed for revealing the microstructure was 30 seconds. Immediately after the immersion finishes, the surface needs to be washed with distilled water and then acetone, before being dried with air. It is important to remember that after the surface is etched and then washed as previously described, the drying process has to be done without direct contact with other materials, in order not to ruin the sample.

4.3.2. Observation of the microstructure

After being etched and dried, the sample is ready to be observed with the optical microscope. Obviously, with an optical microscope we cannot have too many details regarding the microstructure, but it is a good first step in order to have a general idea for what concerns the microstructure. If a second phase is evident, the use of an SEM (Scanning Electron Microscope), which is expensive, can be avoided and another solutionizing process has to be tried. Otherwise, the observation with the SEM and an EDS (Energy Dispersive X-ray Spectroscopy) analysis can be conducted in order to better investigate the microstructure.

A scanning electron microscope is a type of electron microscope that produces images of a sample by scanning it with a focused beam of electrons. The electrons interact with atoms in the sample, producing various signals that can be detected and that contain information about the sample's surface topography and composition.

The EDS analysis is an analytical technique used for the elemental analysis or chemical characterization of a sample. It relies on an interaction of some source of X-ray excitation and a sample.

Before being analyzed with the SEM, the sample required an additional preparation. The lateral surface of the mounted sample has been covered with aluminum foil and the top surface was carbon coated. Both the treatments had the aim of creating a conduction path for the electrons.

Figure 4.9: The microscopes used. On the left, the high quality optical microscope; on the right, the scanning electron microscope

4.4. Hardness measurements

The hardness of a material is a measure of the lattice resistance to the penetration of a specific indenter. A certain load is applied to the indenter and, after a varying holding time, removed, so that the trace of the indentation left on the sample surface indicates how hard the evaluated sample is; of course the higher the hardness the smaller the penetration.

During the test the material undergoes a surface deformation and then dislocations movement is implied. Therefore, since the formation of precipitates hinders dislocations motion which, in turn, results into lower deformation and penetration, the measured hardness values provide a direct idea on the amount and type of precipitates present in the microstructure. For example GPI zones, being small and coherent with the matrix, do not require a lot of energy to be overcome. On the other side, when η' nucleates, dislocations motion is hindered and the material hardness increases.

The relationship between hardness and precipitates is the same as that between strength and precipitates; therefore a direct relationship exists between hardness and strength, both

yield strength and ultimate tensile strength. The relationship between hardness and strength is linear and the angular coefficient is a function of parameters such as the different material analyzed, the material strength, the processes components have been submitted to and the adopted hardness tests [57].
The hardness measurements carried out within this work were done using a Vickers machine, so they can be referred to as microhardness measurements.

4.4.1. Microhardness – Vickers

The Vickers test was chosen to carry out the measurements. For this scale the indenter is characterized by a pyramidal shape, with a squared base, and both the applied load and the holding time can be decided by the user; in this thesis a load of 50 g and a holding time of 12 s were selected.
A typical trace of a Vickers indentation on the material surface is shown in Figure 4.10, where the squared base pyramidal indenter can be recognized.

Figure 4.10: Optical micrograph of a Vickers indentation **[58]**

By knowing the length of the two diagonals and the applied load, the hardness value can be calculated through the equation:

$$HV = 1854 * \frac{F}{l^2} \qquad (4.1)$$

Where HV stands for Hardness Vickers, F is the applied load [g] and l is the arithmetic mean of the two diagonals [µm]. While conducting the tests, the hardness values were not calculated through the formula shown above, but a table was used. Knowing the applied load and calculating the mean of the two diagonals after having measured the two values, the HV can be read from the table.
The machine used for the measurements is reported in Figure 4.11.

Figure 4.11: Buehler Micromet II microhardness testing machine used for the tests

All the possible conditions have been tested with the Vickers machine, repeating the measurement 5 times for each condition in order to obtain an average value with a standard deviation. Proceeding in this way, the curves for each temperature at different ageing times could be observed. The ageing time corresponding to the peak value for each temperature was selected as a condition to be tested with the tensile machine.

4.5. Tensile tests

4.5.1. Tensile tests at room temperature

The heat treatments performed on the coupons which had the highest hardness values were repeated for the specimens prepared for the tensile tests. The tests at room temperature were performed with the machine shown in Figure 4.12.

Figure 4.12: Tensile machine for the tests at room temperature

A template has been created to insert the information regarding the specimens and the type of test required. The machine has a capacity of 50 kN and it has been used with a strain rate of 2 mm/minute. The dimensions (thickness, width) of the specimen were implemented in the template but also checked before each test with the use of a digital caliper.

The information regarding the stress and the strain can be calculated knowing other data coming directly from the software which controls the tensile machine. The stress is easily obtained dividing the load, which is given by the software, by the cross sectional area of the specimen. In order to measure the elongation, an extensometer (gauge length 50 mm)

was placed next to the specimen during the test, as shown in Figure 4.13. From the gauge length and the value of the elongation measured by the extensometer, we can calculate the corresponding strain.

We must say that, in order to have accurate measurements, the load of the tensile machine has to be verified each time the device is started and the correctness of the values given by the extensometer needs to be checked as well.

Figure 4.13: Extensometer in position during the tensile test

After the machine is started, the test goes on until the fracture of the specimen. The data regarding load and elongation are automatically saved by the software, which is also responsible for stopping the machine as soon as the break is detected.

With the aim of avoiding mistakes, each condition was tested three times to see if the behavior of the material was always the same. More samples than necessary were prepared in advance, because it can be expected that some of the tests are not successful, mainly due to the extensometer, which is placed in an instable position which could cause it to rotate around the specimen. In the case the previous scenario occurs, the results are not significant and need to be discarded.

4.5.2. Tensile tests at room temperature after heating

The second typology of tensile test carried out was always at room temperature but after holding the material at different temperatures for 5 minutes. As previously said in chapter 3, this kind of test is very important: the temperature at which a rapid decline in strength begins defines the best, and usually optimum, forming temperature. Moreover, the characteristics of the component after stamping can be understood as well.

According to the literature, a time corresponding to 5 minutes was chosen because it is the maximum holding time expected in a production trial. If, with new technologies, shorter times will be needed, the maximum forming temperature will increase.

Since the warm forming temperature for 7xxx series aluminum alloys is around 200ºC, three different temperatures around that value were chosen: 170ºC, 200ºC and 230ºC. After having selected the temperatures, the procedure to be followed is simple. The specimen has to be placed in the furnace at the desired temperature for five minutes, after that removed and then the tensile test at room temperature can be performed exactly in the same way described in the previous section. Again, the use of an extensometer will be needed for the calculation of the strain and the test stops when the fracture occurs. Tests for each temperature (170, 200 and 230ºC) have been performed in the as received condition and for each ageing temperature at the ageing time that gives the highest hardness value.

4.5.3. Tensile tests at high temperature

The last type of tensile test, performed at high temperature, requires a different equipment to be performed. The temperature selected was 170ºC for two main reasons: at this temperature the mechanical properties of the alloy demonstrated to remain high enough and, from a more practical point of view, a temperature higher than 177ºC would have required major changes to the tensile machine.

The tensile tests at warm forming temperature represent an excellent way for understanding how much the material can be deformed at high temperature, so what is

the maximum elongation that can be expected and with which load, before the specimen breaks (useful also for dimensioning the press). The information gained, combined with the forming limit curves (FLC), is a useful tool that can be used for simulations regarding the formability of the material at high temperature.

The tensile machine operates (the part in which the specimen is placed) inside an environmental chamber, as illustrated in Figure 4.14.

Figure 4.14: Tensile machine with the environmental chamber

A cooling system is necessary in order to prevent possible damages due to overheating of parts of the machine. On the left, in the image it is possible to see the controller of the environmental chamber, through which the temperature can be set. The capacity of the machine is 300 kN and the same template, used for the tests at room temperature with the information related to the specimens, was employed. Again, a strain rate of 2 mm/minute was adopted.

A detail related to the internal part of the environmental chamber is depicted in Figure 4.15.

Figure 4.15 Internal part of the environmental chamber, used for the tensile tests at high temperature

Before starting with the tests, it was important to understand how long it takes for the specimen in order to reach the temperature of the furnace. Some measurements have been conducted, exploiting the use of a thermocouple and a non-contact infrared thermometer. The controller was set to 170ºC. After the temperature inside the environmental chamber reached that value and stabilized, the specimen was placed inside. The temperature of the sample was continuously controlled and the time after which it reaches the temperature found, corresponding to 8 minutes. 10 minutes after having placed the specimen inside the environmental chamber, the test started.

Figure 4.16: On the left, a non-contact infrared thermometer. On the right, a thermocouple.

Also for the tests conducted at high temperature, the same cases mentioned in the previous sections were selected for the experiments.

4.6. Fracture surface analysis

The last step of the experimental work consisted in carrying out a fracture surface analysis with the SEM, in order to understand what kind of fracture occurred. The region around the fracture surface of 4 different specimens tested at room temperature was cut into smaller pieces; the conditions analyzed are the following:

- As received
- Solutionized at 480ºC for 2 hours
- Aged at 120ºC for 20 hours
- Aged at 155ºC for 17 hours

In Figure 4.17 it is shown how the pieces of the specimen that will be analyzed are placed before being inserted in the SEM chamber.

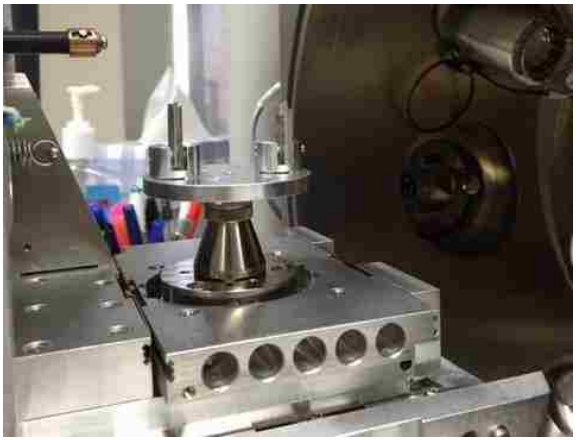

Figure 4.17: samples positioned for the fracture surface analysis with the SEM

When inclusions appear to be evident in the fracture surface, through the EDS elemental analysis, we can discover what elements are present in the inclusion. The inclusions are one of the main causes because of which a crack can start.

5. Results and discussion

In this chapter the results and images coming from the microstructural analysis are shown. The curves resulting from the hardness measurements and tensile tests are illustrated and discussed. At the end of the section, the fracture surface analysis is reported.

5.1. Microstructural observation and EDS analysis

The first section of the results is dedicated to the discussion of the images captured with the optical microscope, at first, and then with the scanning electron microscope. Also, the data coming from the EDS analysis, in which the elements present in the microstructure are highlighted, are reported and explained. The objective of the microstructural analysis is to verify, for what concerns the solutionized sample, if the solutionizing process occurred properly, so a second phase should not be present in the microstructure. The solutionizing adopted, as mentioned in chapter 4, consisted in holding the material in a furnace at 480ºC for 2 hours. A quenching in icy water followed. It must be kept in mind that, in any case, an SEM analysis is still not enough if there is the need to observe the precipitates. In that, case a TEM (transmission electron microscope) analysis should be carried out; this is expensive and requires a bigger effort for the sample preparation.

5.1.1. Optical microscope images

As previously mentioned in chapter 4, the samples for the observation with the optical microscope need to be polished and etched before the analysis. Since the material is an aluminum alloy, softer compared to many other metals, the elimination of all the scratches is not a trivial process and requires a careful treatment. During the last stages of

polishing, a polishing cloth with alumina was used in order to remove also the smallest scratches from the surface.

Another important parameter that has to be set correctly is the etching time. After having identified the etchant that reveals in the best way the microstructure, the time of exposure has to be established. An immersion of the sample in the solution for a time that is not sufficient does not reveal the grain boundaries in a clear way. On the other hand, if the sample is hold for too long in the etchant, the surface becomes "burnt" and it cannot be observed. In order to understand which immersion time corresponds to the optimum value for the etchant, a trials and errors procedure has to be followed. Practically, if with the microscope we see the grain boundaries not well defined and they disappear from certain regions of the microstructure, the time of exposure is not enough. On the other hand, if what we observe is a surface that looks very black and nothing can be really distinguished, the holding time was too long.

The images were taken with the optical microscope at different magnifications. The analysis was repeated both for the material in the as received condition and after solutionizing (in the furnace at 480ºC for 2 hours).

In the Figure 5.1, we can see the microstructure of the solutionized sample:

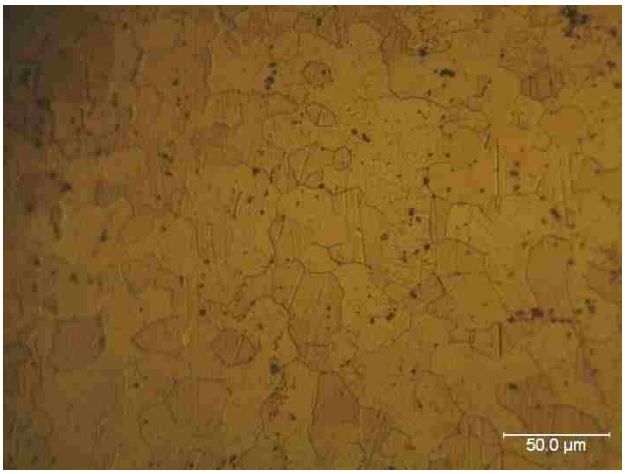

Figure 5.1: Optical microscope image of the aluminum alloy 7046, solutionized at 480 ºC for 2 hours. The microstructure was revealed with immersion in the Kellers etchant for 30 seconds.

As can be seen from the picture, the grain boundaries are well defined and, at a first sight, we cannot see the presence of a second phase. The smaller black dots and the conglomerates that we can see areporosities, as will be evidenced by the SEM analysis.
Since, according to the results obtained with the optical microscope, the surface appears to be properly solutionized, the analysis with the SEM can be performed in order to have more details on the microstructure.

5.1.2. Scanning electron microscope images

The sample used for the SEM analysis is exactly the same prepared for the optical microscope, in which a conducting path for the electrons is built as described in chapter 4.
Also in this case the images where taken at different magnifications and, after that, an EDS analysis was performed in order to understand the elements present in specific regions of the microstructure.

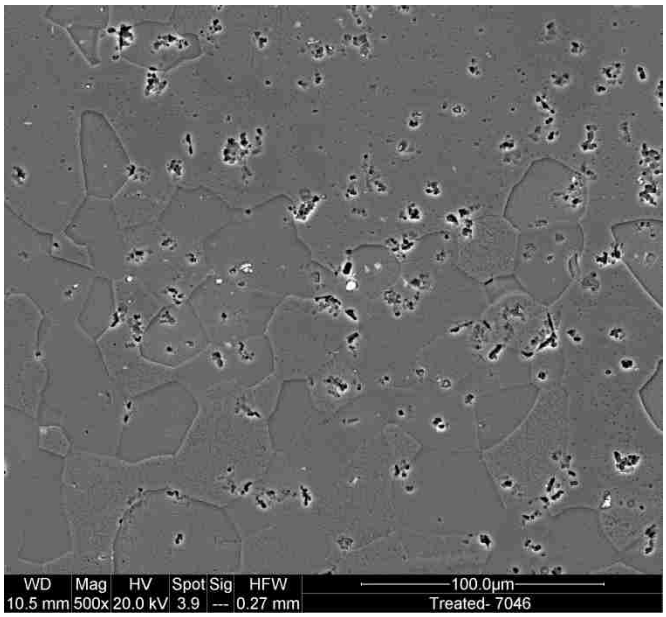

Figure 5.2: SEM image of the aluminum alloy 7046, solutionized at 480 ºC for 2 hours. The microstructure was revealed with immersion in the Kellers etchant for 30 seconds.

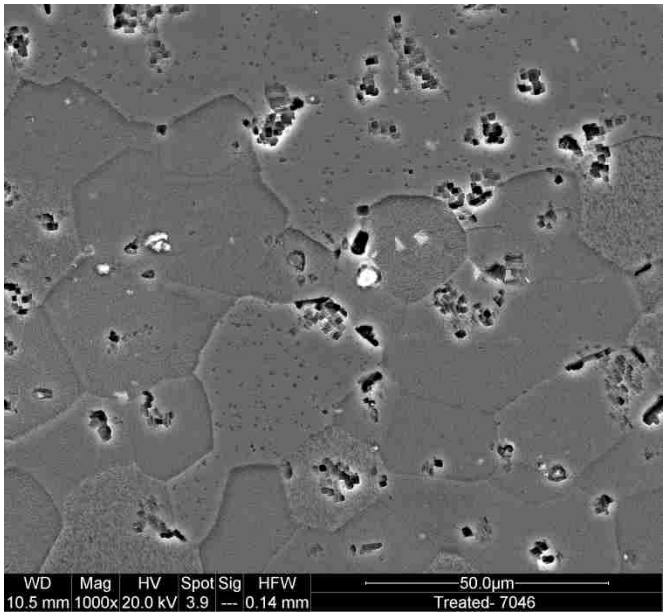

Figure 5.3: SEM image of the aluminum alloy 7046, solutionized at 480 ºC for 2 hours. The microstructure was revealed with immersion in the Kellers etchant for 30 seconds

From Figure 5.2 and Figure 5.3, it can be noticed that the aluminum matrix appears to be homogeneous. The black spots, seen also with the optical microscope, are visible and in particular regions white zones are present as well. With a higher magnification, some of the bigger black spots were investigated. They are porosities in the metal matrix..
In order to understand which elements are present in the matrix and in the brighter and darker spots, the elemental analysis was carried out.

5.1.3. EDS analysis

A certain region of the microstructure, observed with the SEM, was selected for an EDS (energy dispersive X-ray spectroscopy) analysis. In Figure 5.4, Figure 5.5 and Figure 5.6 the spots identified for the analysis are reported.

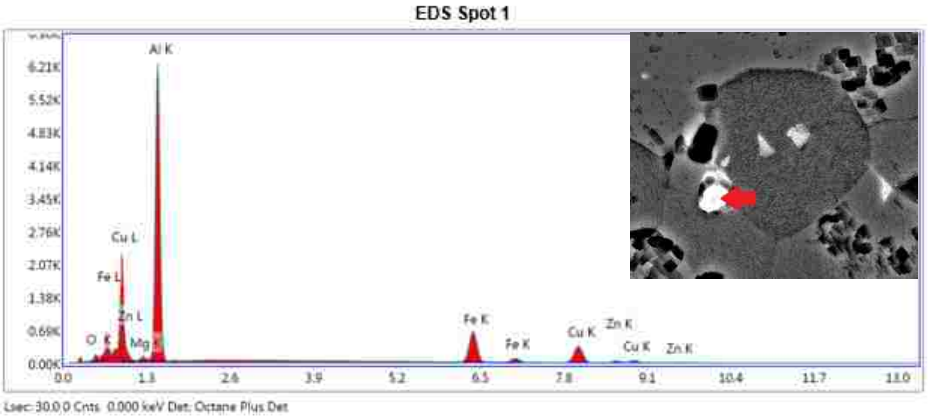

Element	Weight %	Atomic %
MgK	0.48	0.69
AlK	52.97	68.15
FeK	19.80	12.31
CuK	21.37	11.68
ZnK	2.74	1.45

Figure 5.4: EDS analysis results for Spot 1, indicated by the red arrow in the picture. The analysis was conducted on the aluminum alloy 7046 solutionized at 480 ºC for 2 hours. The elements found are first highlighted with the peaks in the diagram and then summarized in the table.

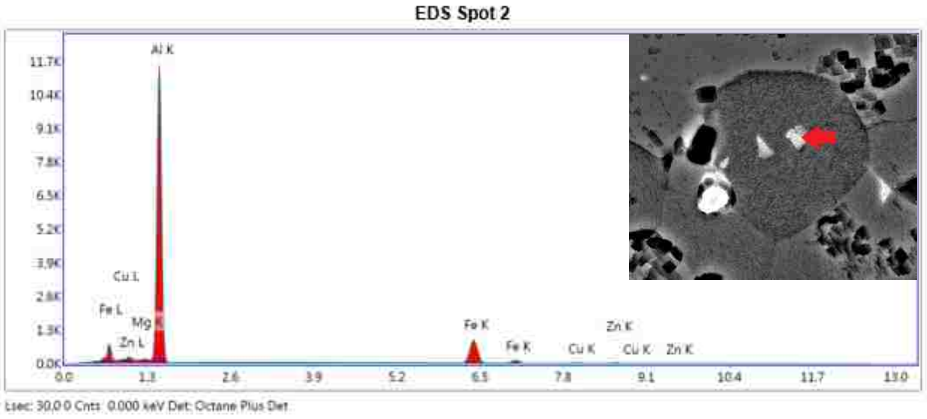

Element	Weight %	Atomic %
MgK	0.81	1.07
AlK	68.75	81.76
FeK	26.39	15.16
CuK	1.70	0.86
ZnK	2.35	1.15

Figure 5.5: EDS analysis results for Spot 2, indicated by the red arrow in the picture. The analysis was conducted on the aluminum alloy 7046 solutionized at 480 ºC for 2 hours. The elements found are first highlighted with the peaks in the diagram and then summarized in the table.

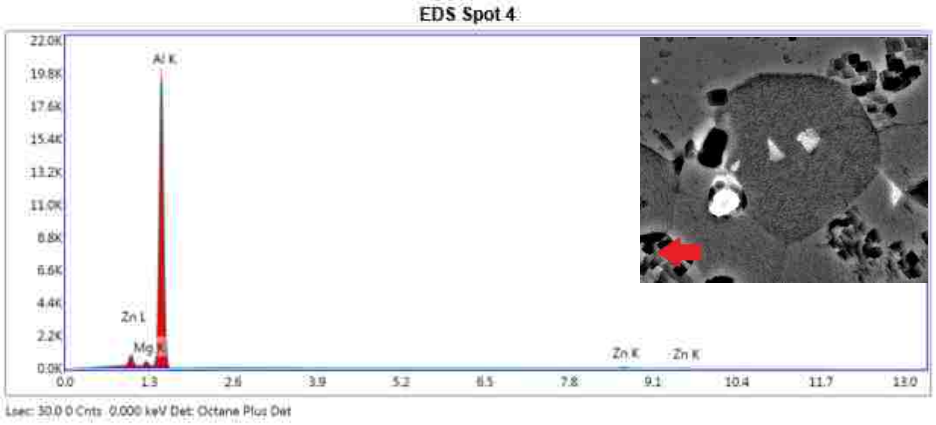

Element	Weight %	Atomic %
MgK	1.76	2.03
AlK	91.41	95.04
ZnK	6.83	2.93

Figure 5.6: EDS analysis results for Spot 4, indicated by the red arrow in the picture. The analysis was conducted on the aluminum alloy 7046 solutionized at 480 ºC for 2 hours. The elements found are first highlighted with the peaks in the diagram and then summarized in the table.

The results for other spots and areas analyzed are not reported since they are redundant. The elements present in those regions are the same as in spot 4 and the weight percentage is more or less equal too. We can understand that the brighter spots are characterized by the presence of iron or copper, while all the other parts (porosities included) have just the elements which characterize the alloy composition.

According to the outcome of the analysis, the microstructure can be considered as homogeneous and it can be said that the solutionizing occurred properly, despite the presence of isolated regions with a high weight percentage of iron or copper. These areas are not spread all over the microstructure with continuity; the dissolution of the second phases is good enough in order to proceed with the ageing treatments.

5.2. Hardness results

Within this section the results coming from the microhardness measurements, conducted with the Vickers microhardness tester, are shown and discussed. At first, just five different ageing times for each ageing temperature were planned. After the tests, looking at the trends obtained, it was noticed that probably the peak value for the ageing temperatures 120ºC and 155ºC was in the interval between 14 and 24 hours. For this reason, other two ageing times were added: 17 and 20 hours, which were not used for the material artificially aged at 185ºC, because it already overages after 14 hours.

The tests were conducted with a load of 50 gf applied for 12 seconds. After having measured the length of the two diagonals created by the indenter, the average value was calculated. Each condition was tested 5 times and the standard deviation calculated.

The results are shown in the diagrams and summarized with the corresponding values of the standard deviation in the tables.

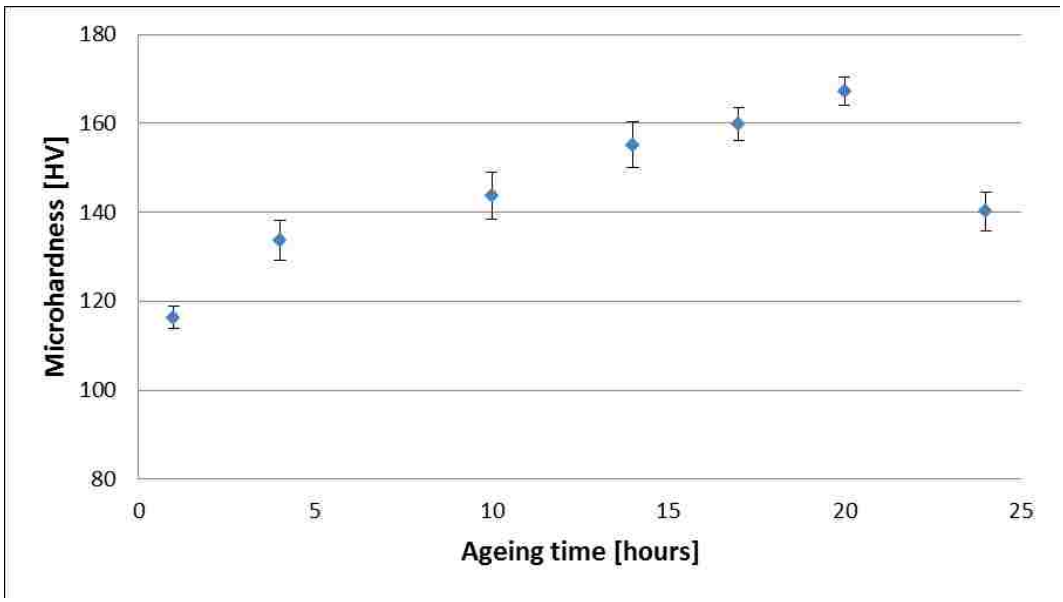

Figure 5.7: Microhardness variation vs. ageing time of the aluminum alloy 7046 aged at 120ºC. The applied load is 50 gf for 12 seconds. Each point on the diagram is the average of 5 different measurements.

Table 5.1: Summary of the hardness values and the corresponding standard deviations for aluminum alloy 7046 aged at 120ºC . The applied load is 50 gf for 12 seconds. Each microhardness value is the average of 5 different measurements, on the base of which the standard deviation is calculated.

Time [hours]	Average hardness [HV]	Standard Deviation
1	116.4	4.98
4	133.8	8.98
10	143.8	10.57
14	155.2	10.33
17	159.8	7.26
20	167.2	6.30
24	140.2	8.79

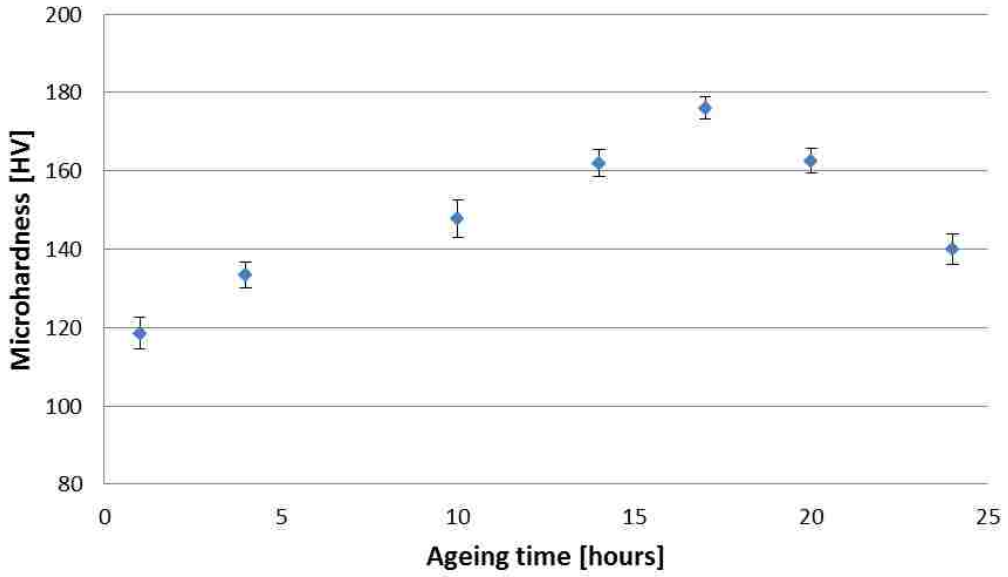

Figure 5.8: Microhardness variation vs. ageing time of the aluminum alloy 7046 aged at 155ºC. The applied load is 50 gf for 12 seconds. Each point on the diagram is the average of 5 different measurements.

Table 5.2: Summary of the hardness values and the corresponding standard deviations for the aluminum alloy 7046 aged at 155ºC. The applied load is 50 gf for 12 seconds. Each microhardness value is the average of 5 different measurements, on the base of which the standard deviation is calculated.

Time [hours]	Average hardness [HV]	Standard Deviation
1	118.6	8.20
4	133.4	6.80
10	147.8	9.50
14	162	6.96
17	176	5.61
20	162.6	6.31
24	140	8.03

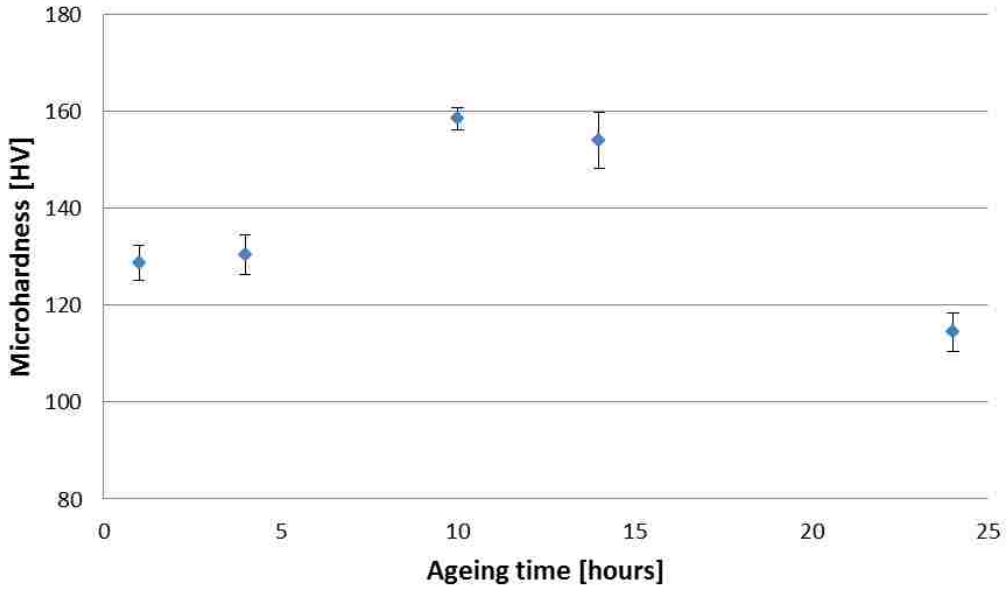

Figure 5.9: Microhardness variation vs. ageing time of the aluminum alloy 7046 aged at 185ºC. The applied load is 50 gf for 12 seconds. Each point on the diagram is the average of 5 different measurements.

Table 5.3: Summary of the hardness values and the corresponding standard deviations for the aluminum alloy 7046 aged at 185ºC. The applied load is 50 gf for 12 seconds. Each microhardness value is the average of 5 different measurements, on the base of which the standard deviation is calculated.

Time [hours]	Average hardness [HV]	Standard Deviation
1	128.8	7.22
4	130.4	8.02
10	158.4	4.45
14	154	11.49
24	114.4	7.89

For each ageing temperature, it is clear how the hardness increases with time for the first period until it reaches a peak, after which the value decreases since the overageing starts with the formation of η (as seen in the literature).

Again, according to what was found in previous studies focused on the precipitation process for 7xxx series aluminum alloy, the peak strength is reached with the formation of η', which nucleates only during artificial ageing.

The ageing time corresponding to the peak is different depending on the temperature at which the material is hold. The ageing process is slower at lower temperatures, while it increases its speed with higher temperatures. It can be seen, indeed, that at 120ºC we have the peak value after 20 hours, while at 185ºC the highest hardness is reached after 10 hours.

Considering the results reported in the previous tables, the ageing times which give the highest hardness values for each ageing temperature are:

- 20 hours for 120ºC, with an average hardness of 167.2 HV
- 17 hours for 155ºC, with an average hardness of 176 HV
- 10 hours for 185ºC, with an average hardness of 158.4 HV

The conditions reported above were chosen to be tested with the tensile machine, together with the as received and solutionized conditions.

5.3. Tensile tests results

At this point, the results coming from the tensile tests can be analyzed. It is important to remember that the experimental work for this part was conducted in three different ways:

- Tensile tests at room temperature, without a previous heating
- Tensile tests at room temperature, after the material was heated up to 3 different temperatures for 5 minutes
- Tensile tests performed at high temperature with the employment of an environmental chamber

The same template, containing the information regarding the specimens, was used for all the tests. The strain rate adopted was 2 mm/minute. The test goes on until a break is detected and the software automatically saves the data which are useful in order to calculate stress and strain.

5.3.1. Tensile tests at room temperature

In the graphs and tables the results coming from the tensile tests conducted at room temperature without being previously heated are shown.

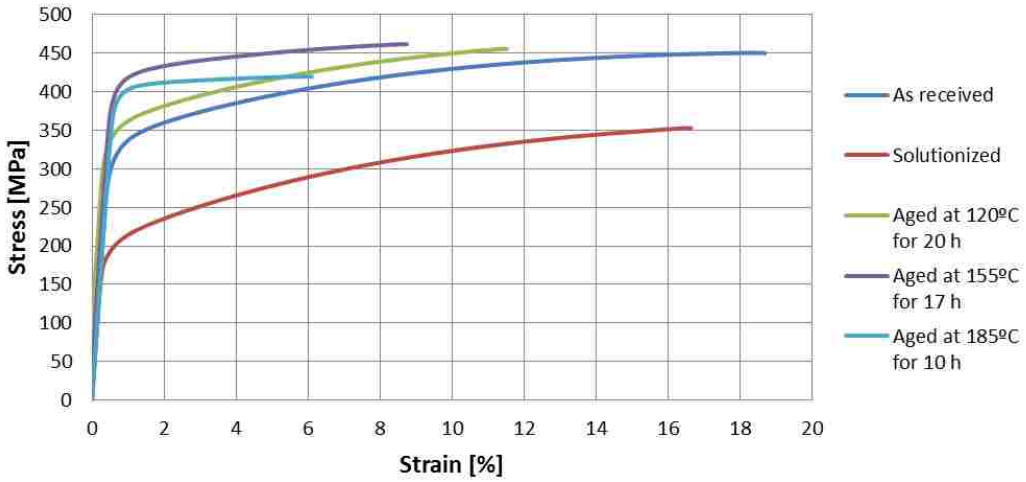

Figure 5.10: Stress-strain diagrams for the tensile tests carried out at room temperature. Aluminum alloy 7046 tested after being aged in 3 different ways, in the as received condition and solutionized at 480 ºC for 2 hours.

From Figure 5.10, there are some considerations that can be done:

- The heat treatment which gives the best UTS is the one performed at 155ºC for 17 hours.
- The ageing at 120ºC for 20 hours improves the UTS compared to the as received condition and shows a better elongation compared to the ageing at 155ºC for 17 hours.
- For what concerns the heat treatment performed at 185ºC for 10 hours, it can be seen that in this case the material does not work harden as much as in the other cases. The UTS is lower than the one of the material in the as received condition but the yield strength, instead, is higher.

- The alloy in the as received condition performs very well in elongation, showing anyway a good behavior also for what concerns the UTS.

The properties of the alloy in each condition tested are summarized in the following table:

Table 5.4: Summary of the properties resulting from the tensile tests carried out at room temperature. Aluminum alloy 7046 tested after being aged in 3 different ways, in the as received condition and solutionized at 480 ºC for 2 hours.

Room temperature			
	UTS [Mpa]	Yield strength [MPa]	Elongation [%]
Aged at 120ºC for 20 hours	455	352	12
Aged at 155ºC for 17 hours	461	414	8.8
Aged at 185ºC for 10 hours	418	395	6
As received	449	321	19
Solutionized	352	203	17

It has to be mentioned that we do not have many details regarding the treatments which underwent the alloy in the as received condition. It has a very good combination of ultimate tensile strength and elongation, which is unusual for something that has been age hardened. Of course, the solutionized condition shows low yield strength and UTS, with a good elongation, which is what can be expected.

Having a look at the results coming from the ageing treatments proposed, in two cases the UTS has been improved with respect to the as received condition. For what concerns the yield strength, instead, the value is higher also for the material aged at 185ºC, but in this case the alloy does not work harden and so the ultimate tensile strength does not have a high value.

5.3.2. Tensile tests at room temperature, alloy previously heated

This section is dedicated to the results obtained from the tensile tests performed after the material was heated for 5 minutes. The procedure followed is the following:

- The material is placed in the furnace at a certain temperature for five minutes. The temperatures chosen were 170, 200 and 230ºC.
- No quenching is performed, the material cools down at room temperature and the waiting time, before proceeding with the tensile test, was 30 minutes. In this way, the material reaches the temperature of the environment in the whole thickness.
- The tensile test is performed.

Thanks to the data obtained, the optimum warm forming temperature can be selected and the final characteristics of the component after stamping found. The temperature at which a rapid decline in strength begins define the maximum, and usually optimum, forming temperature. The diagrams for each heating temperature chosen with the tables which summarize the properties are reported.

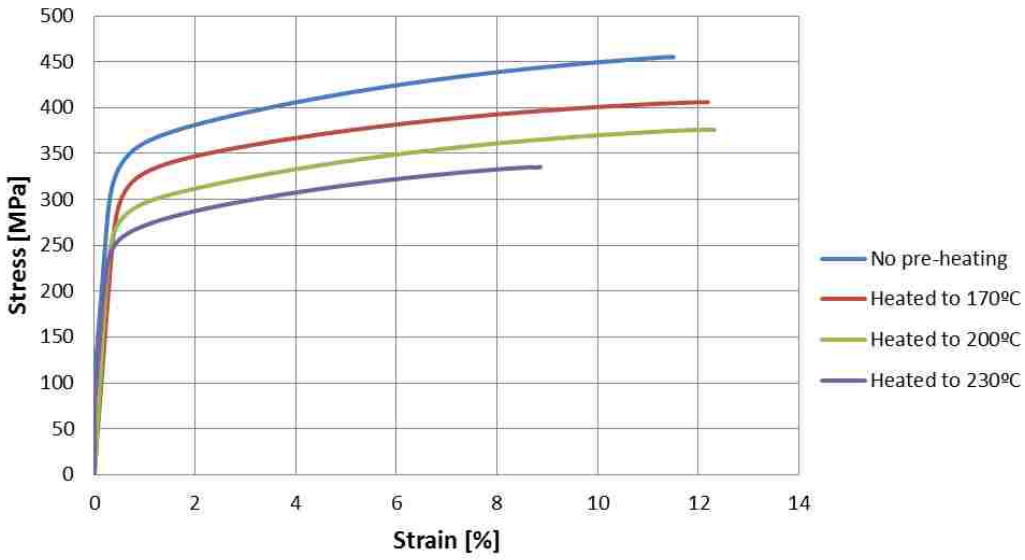

Figure 5.11: Stress-strain diagrams for the tensile tests carried out at room temperature on the aluminum alloy 7046 aged at 120 ºC for 20 hours. 3 of the 4 curves show the behavior of the alloy after it was previously heated to different temperatures (170, 200 and 230 ºC) for 5 minutes.

Table 5.5: Summary of the properties resulting from the tensile tests carried out at room temperature on the aluminum alloy 7046 aged at 120 ºC for 20 hours. 3 of the 4 conditions show the behavior of the alloy after it was previously heated to different temperatures (170, 200 and 230 ºC) for 5 minutes.

Aged at 120ºC for 20 hours			
	UTS [Mpa]	Yield strength [MPa]	Elongation [%]
No pre-heating	455	352	12
Heated to 170ºC	406	318	12.3
Heated to 200ºC	376	280	12.4
Heated to 230ºC	335	258	9

.

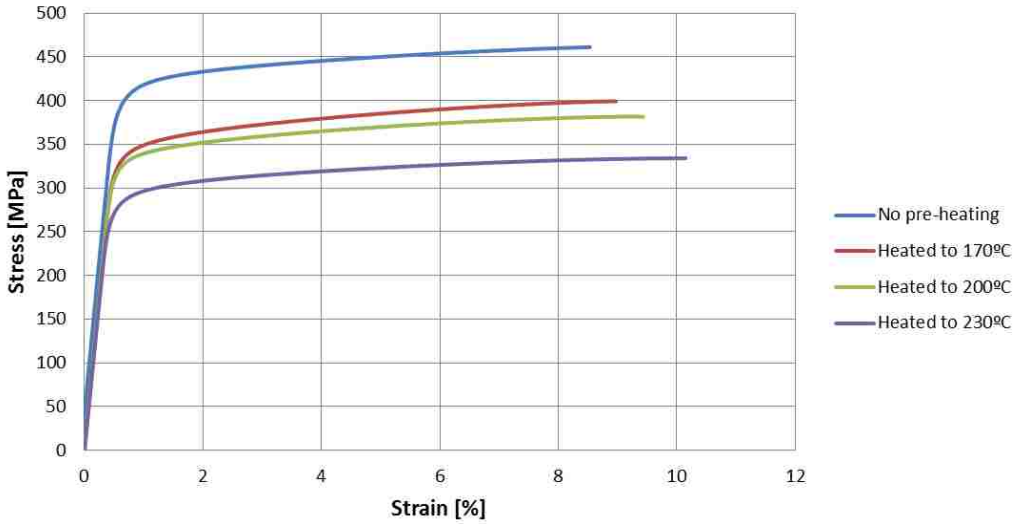

Figure 5.12: Stress-strain diagrams for the tensile tests carried out at room temperature on the aluminum alloy 7046 aged at 155 ºC for 17 hours. 3 of the 4 curves show the behavior of the alloy after it was previously heated to different temperatures (170, 200 and 230 ºC) for 5 minutes.

Table 5.6: Summary of the properties resulting from the tensile tests carried out at room temperature on the aluminum alloy 7046 aged at 155 ºC for 17 hours. 3 of the 4 conditions show the behavior of the alloy after it was previously heated to different temperatures (170, 200 and 230 ºC) for 5 minutes.

Aged at 155ºCfor 17 hours			
	UTS [Mpa]	Yield strength [MPa]	Elongation [%]
No pre-heating	461	414	8.8
Heated to 170ºC	399	333	9.2
Heated to 200ºC	381	330	9.8
Heated to 230ºC	334	287	10.7

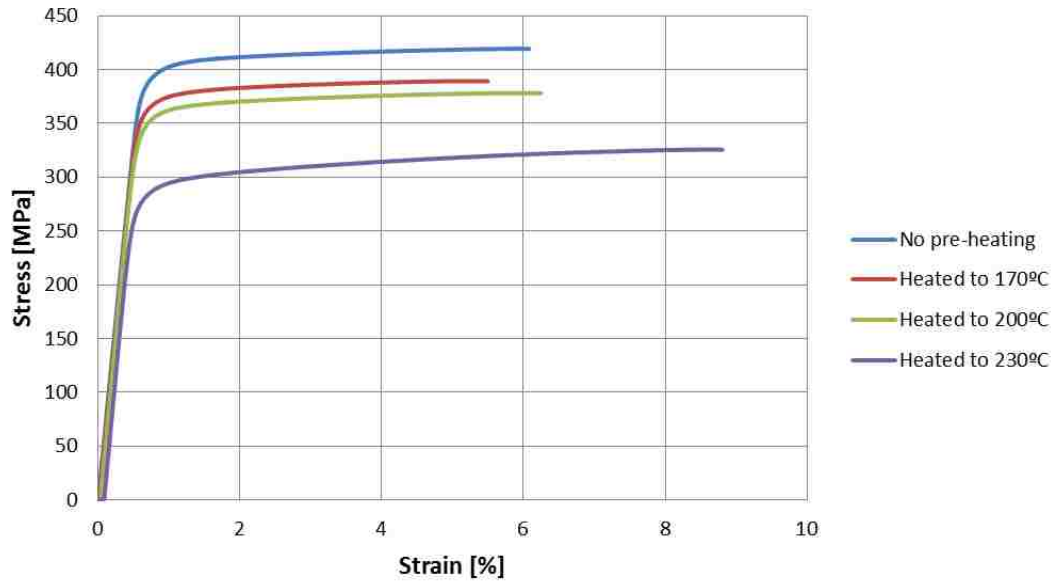

Figure 5.13: Stress-strain diagrams for the tensile tests carried out at room temperature on the aluminum alloy 7046 aged at 185 ºC for 10 hours. 3 of the 4 curves show the behavior of the alloy after it was previously heated to different temperatures (170, 200 and 230 ºC) for 5 minutes.

Table 5.7: Summary of the properties resulting from the tensile tests carried out at room temperature on the aluminum alloy 7046 aged at 185 ºC for 10 hours. 3 of the 4 conditions show the behavior of the alloy after it was previously heated to different temperatures (170, 200 and 230 ºC) for 5 minutes.

Aged at 185ºC for 10 hours			
	UTS [Mpa]	Yield strength [MPa]	Elongation [%]
No pre-heating	418	395	6
Heated to 170ºC	389	360	5.9
Heated to 200ºC	378	357	7.7
Heated to 230ºC	325	288	9.4

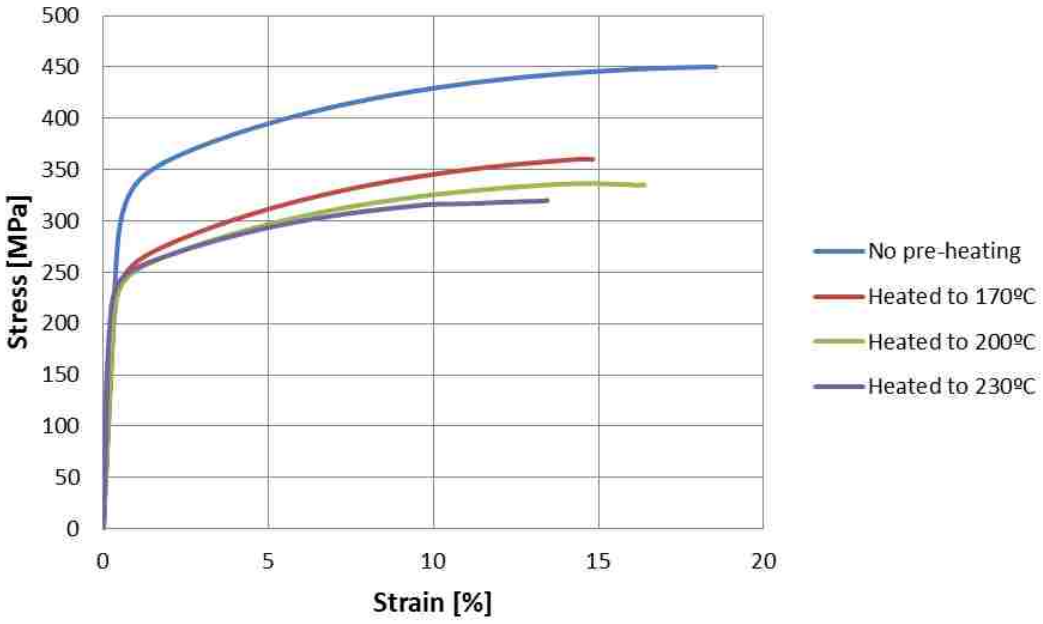

Figure 5.14: Stress-strain diagrams for the tensile tests carried out at room temperature on the aluminum alloy 7046 as received. 3 of the 4 curves show the behavior of the alloy after it was previously heated to different temperatures (170, 200 and 230 ºC) for 5 minutes.

Table 5.8: Summary of the properties resulting from the tensile tests carried out at room temperature on the aluminum alloy 7046 as received. 3 of the 4 conditions show the behavior of the alloy after it was previously heated to different temperatures (170, 200 and 230 ºC) for 5 minutes.

As received			
	UTS [Mpa]	Yield strength [MPa]	Elongation [%]
No pre-heating	449	321	19
Heated to 170ºC	360	251	15.8
Heated to 200ºC	336	233	17
Heated to 230ºC	320	231	13.5

Some considerations can be drawn from the results shown in the previous diagrams and tables:

- As it could be imagined, the properties of the alloy undergo a decay increasing the temperature at which it is exposed for 5 minutes. This is valid for the alloy in the as received condition but also for each treatment performed.
- When the material is heated up to 170ºC, the UTS decreases more for the alloy as received compared to the treated conditions.

- The best elongation is always given by the as received condition, but with the ageing performed at 120ºC the UTS and yield strength are higher maintaining in any case a good elongation.
- The alloy artificially aged at 185ºC for 10 hours does not work harden in a good way, exactly as it was found after the tests at room temperature without pre-heating.
- The heat treatment at 155ºC for 17 hours, which gives the best UTS at room temperature if not previously heated, shows a higher decay in the mechanical properties if heated and does not work harden as properly as the ageing conducted at 120ºC for 20 hours.

5.3.3. Tensile tests at high temperature

The last type of tensile tests performed required the adoption of a different machine, which had to be combined with an environmental chamber in order to carry out the tests at higher temperatures.
The results, in this case, are important for having an understanding on the behavior of the material at high temperature. Some of the characteristics that can be studied:

- The deformability of the alloy
- The maximum elongation reachable before a break occurs
- The stress at which the failure verifies

Thanks to the gained information, simulations for the formability of the material at high temperature could be done.

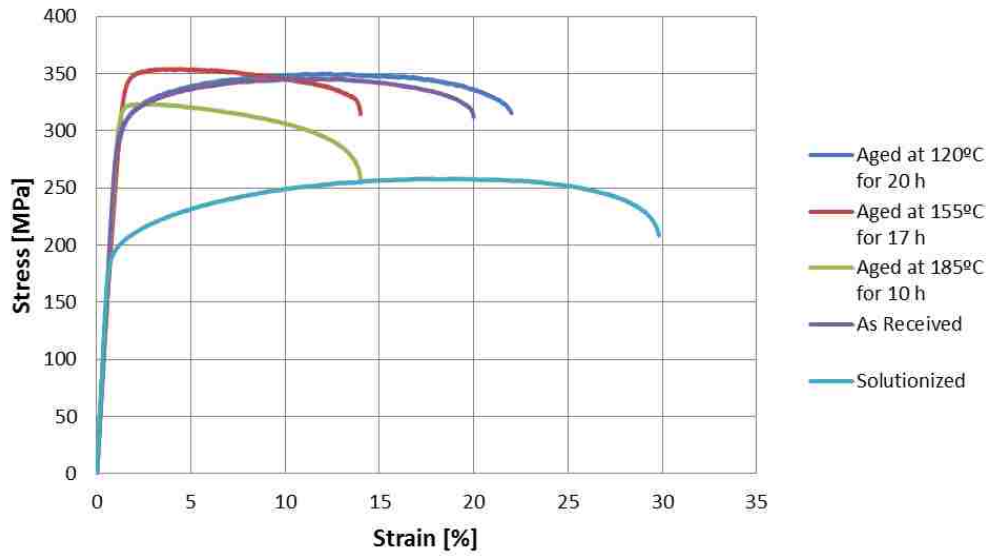

Figure 5.15: Stress-strain diagrams for the tensile tests carried out at 170 ºC on the aluminum alloy 7046, for each condition tested: 3 different ageing conditions, as received and solutionized at 480ºC for 2 hours.

As can be clearly understood from the curves in the graph shown in Figure 5.15, the stress-strain curves of the results refer to the engineering stress and strain and not to the true stress and strain. This is the reason why the curves, after a while, go down to level of stress (and so also level of load) lower compared to the peak values. The explanation is quite simple: in the engineering stress, the area over which the stress is calculated is always the initial area. In this way, it does not take into account that an area reduction is present during the test, due to the fact that the specimen is elongating.

During the tests at high temperature, the elongation is much higher compared to the one obtained from the tests at room temperature, the necking phenomenon is accentuated and visible, so the curve goes down as it is shown by the figure.

Table 5.9: Summary of the properties resulting from the tensile tests carried out at 170 ºC, for each condition tested: 3 different ageing conditions, as received and solutionized at 480ºC for 2 hours.

Tensile tests at high temperature			
	UTS [Mpa]	Yield strength [MPa]	Elongation [%]
Aged at 120ºC for 20 hours	349	296	22
Aged at 155ºC for 17 hours	353	345	14
Aged at 185ºC for 10 hours	323	322	14
As received	345	295	20
Solutionized	258	184	30

- Of course, the condition which gives the best elongation is the solutionized alloy, which is also the one with the lowest UTS and yield strength.
- The best compromise between strength and elongation is given by the material treated at 120ºC for 20 hours.
- In this case, the as received condition does not show the best possible elongation (solutionized condition excluded), which is instead given by the material aged at 120ºC for 20 hours (22%).
- The best UTS is again given by the alloy aged at 155ºC for 17 hours, but the elongation is not so elevated and in this case the UTS given by the ageing at 120ºC for 20 hours is very close.
- The values regarding the ultimate tensile strength and yield strength are lower compared to what it was obtained at room temperature, and this is something that can be easily expected.
- Depending on what are the properties needed by the material, a certain treatment can be chosen instead of another one.

5.4. Microstructural analysis of fracture surfaces

The last step of the experimental work consisted in a fracture surface analysis, performed with the scanning electron microscope. The objective of this analysis is to evaluate the micromechanisms of fracture.

The fracture surface of samples tested by loading at room temperature were:

- As received
- Solutionized for 2 hours at 480ºC
- Aged at 155ºC for 17 hours
- Aged at 120ºC for 20 hours

Figure 5.16 shows the solutionized condition and Figure 5.17 the material aged at 155ºC. Then, the other conditions will be shown and the EDS analysis performed on an inclusion reported.

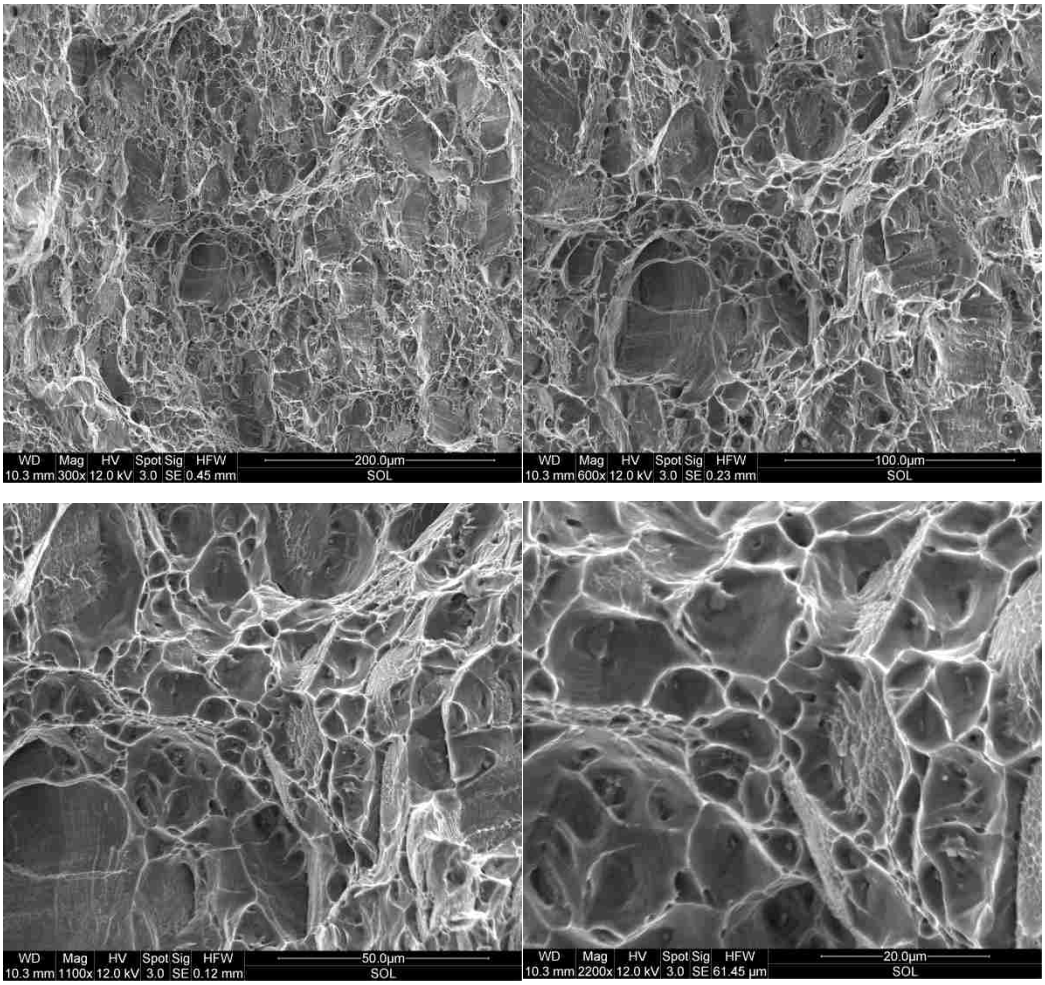

Figure 5.16: SEM images of the aluminum alloy 7046 solutionized at 480ºC for 2 hours, different magnifications of the same region. The fracture is very ductile as evidenced by the presence of dimples clearly visible.

The dimples present in the SEM images reported in Figure 5.16 are evident, the fracture occurred in a ductile way.

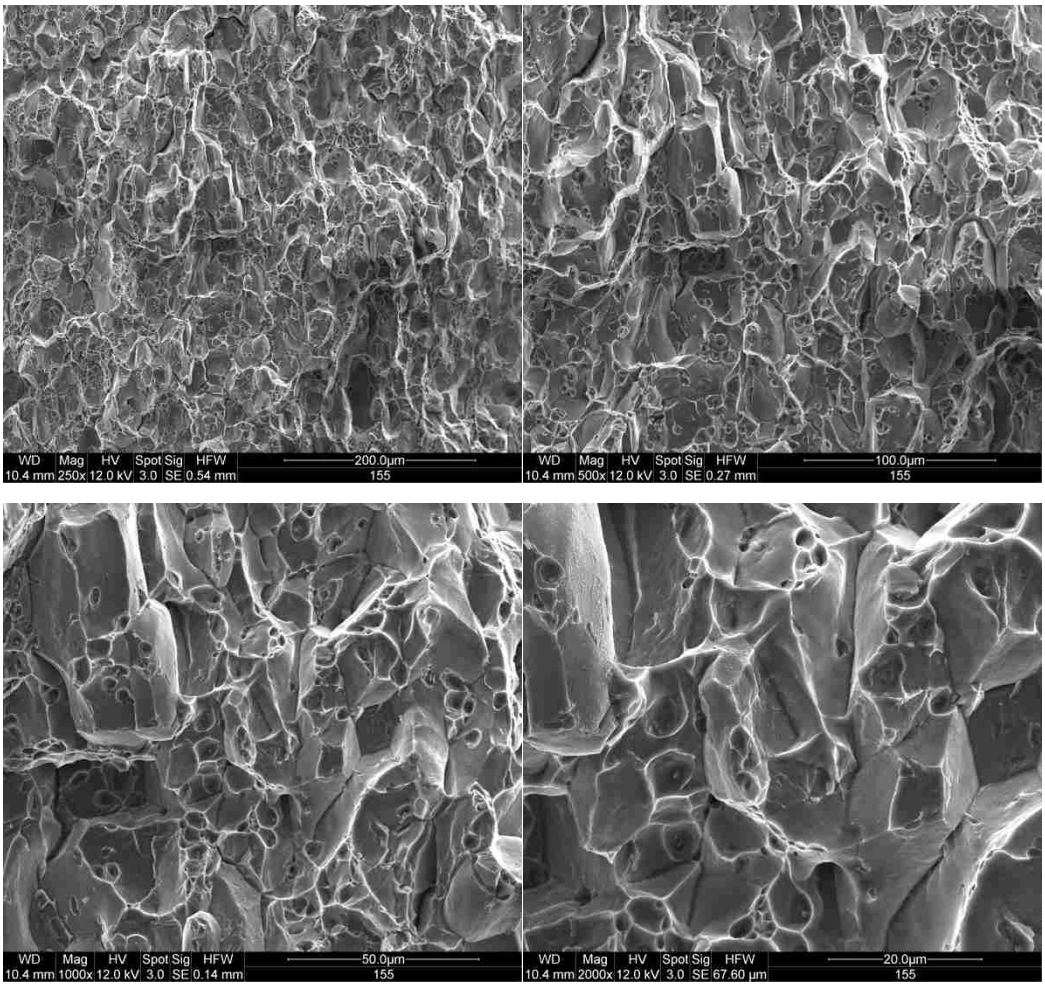

Figure 5.17: SEM images of the aluminum alloy 7046 aged at 155 ºC for 17 hours, different magnifications of the same region. In this case the fracture is brittle.

Fig 5.17 shows a transgranular type of fracture which failed in a brittle manner. Some dimples are still visible but they are much more evident in the solutionized condition (at 480ºC for 2 hours). If the solutionizing is not followed by ageing, the hardness of the material is lower and so it elongates more before fracturing.

Figure 5.18 and Figure 5.19 refer to the alloy in the as received condition. Three different magnifications are reported and also a bigger image which covers a wider area is present.

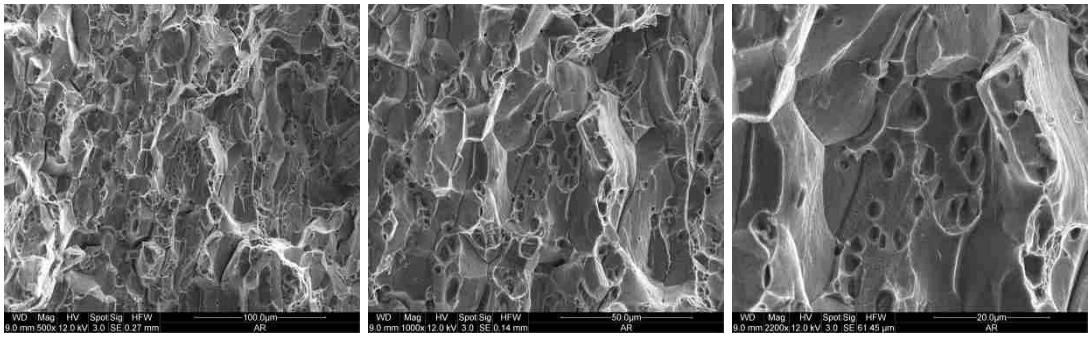

Figure 5.18: Three different magnifications of the fracture surface of the aluminum alloy7046 in the as received condition. The fracture can be classified as brittle.

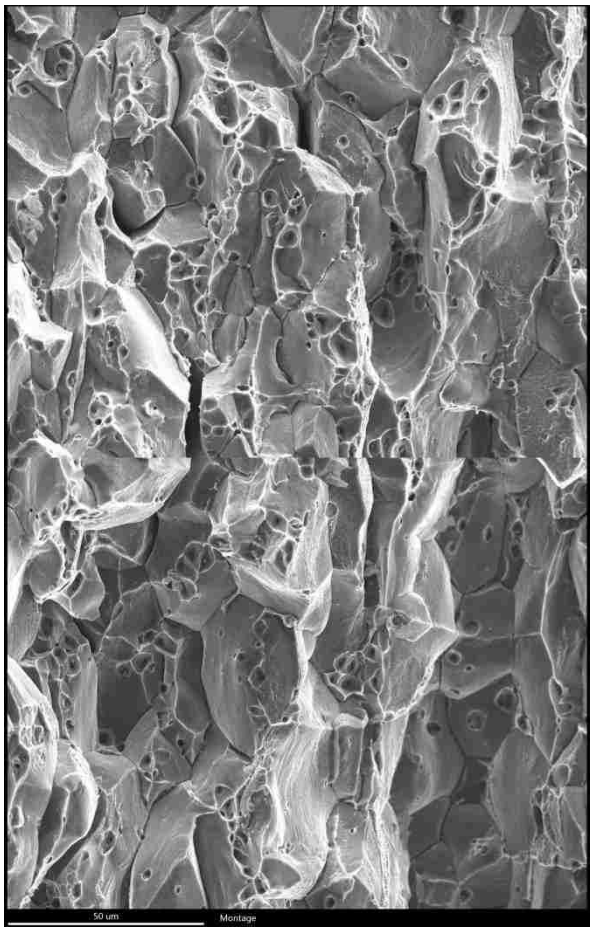

Figure 5.19: SEM image of the fracture surface of the aluminum alloy 7046 in the as received condition.

The last condition shown is the one aged at 120ºC for 20 hours. In this case an inclusion was identified and an EDS analysis performed onto it in order to understand which elements were present.

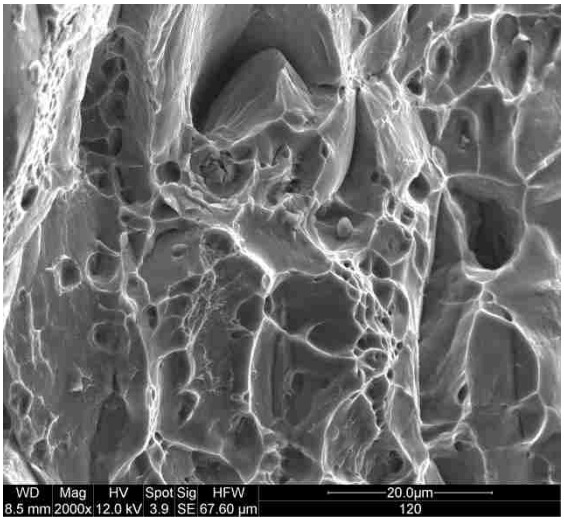

Figure 5.20: SEM image of the aluminum alloy 7046 aged at 120ºC for 20 hours. Ductile fracture with dimples.

In this case, the dimples are clear and so the fracture occurred in a ductile way. As previously mentioned, inclusions or second phase particles can act as microvoid initiation sites. They lose coherency with the matrix forming a microvoid around each particle. After a while, when a load is applied (in this case during the tensile test), the expansion of microvoids leads to their coalescence, giving the complete failure.

In Figure 5.21, the blue arrow identifies the inclusion onto which the EDS analysis was performed.

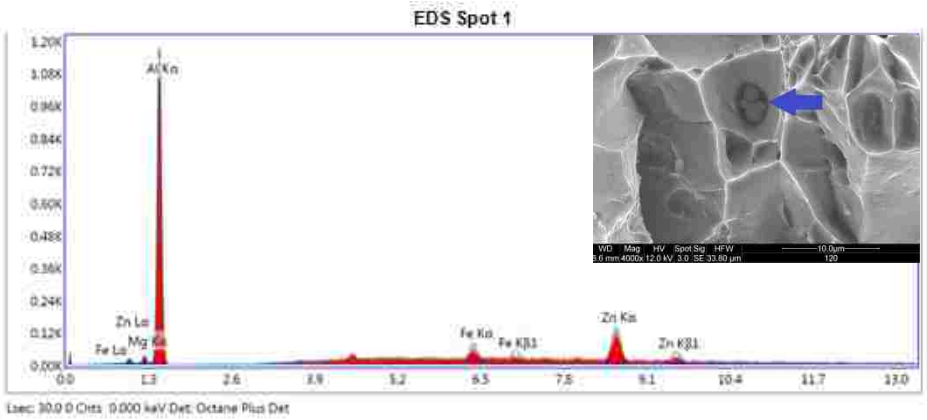

Element	Weight %	Atomic %
MgK	1.79	2.77
AlK	49.20	68.36
FeK	7.89	5.29
ZnK	41.11	23.58

Figure 5.21: Results of the EDS analysis conducted on the inclusion found in the fracture surface of the aluminum alloy 7046 aged at 120ºC for 20 hours. The inclusion is highlighted with the blue arrow in the image. The specimen underwent a tensile test at room temperature.

The EDS analysis, in order to have a comparison, was performed also in other spots of the region. The results for the other spots are not reported since nothing particular was found, the elemental analysis highlighted the presence of aluminum, zinc and magnesium in the expected amounts.

For what concerns the inclusion, instead, we can see the presence of iron in a not negligible percentage. As can be seen from the image, the inclusion is in the middle of the microvoid, as almost always happens.

5.5. Discussion

In this last section of the chapter, a discussion of the results is given in order to summarize what was obtained.

The first part of the experimental work was focused on the definition of a solutionizing process which allows having only one phase in the microstructure. The microstructural analysis was carried out first with an optical microscope and then with an SEM. As can be seen in section 5.1, the presence of a second phase was excluded after the solutionizing at 480ºC for 2 hours, which was therefore adopted as the first step of the precipitation hardening process. The microstructure shown in Figure 5.3 shows a homogeneous composition; only two spots (onto which an EDS analysis was performed, Figure 5.4 and Figure 5.5) demonstrated to have a high percentage of iron and copper. These spots are isolated and so their presence is not enough for saying that the solutionizing process did not occur properly.

The first common part of the treatment was followed by 3 different ageing processes at the following temperatures: 120, 155 and 185ºC. Several ageing times have been tried for each ageing temperature and the hardness was measured after each trial. In order to perform a more accurate measurement, each condition was tested 5 times with the Vickers machine and the average value of the hardness calculated. The ageing time which gave the best result was identified (as a reference, these results can be found in Table 5.1, Table 5.2 and Table 5.3) for each ageing temperature. In this way, 3 different ageing procedures were identified:

- At 120ºC for 20 hours
- At 155ºC for 17 hours
- At 185ºC for 10 hours

The abovementioned conditions were studied, focusing on the tensile properties of the aluminum alloy 7046. The experimental work in this phase was divided into three different parts. The first one consisted in tensile tests conducted at room temperature, after that the same tests were performed with the alloy previously heated at different

temperatures for 5 minutes and finally the tensile tests at high temperature were performed.

Considering the tensile tests conducted at room temperature (Figure 5.10 and Table 5.4):

- Two of the three precipitation hardening processes improved the ultimate tensile strength of the alloy with respect to the as received condition: alloy artificially aged at 120ºC for 20 hours and at 155ºC for 17 hours.
- It must be kept into account that the alloy in the as received condition was already treated, but not many details were known about the heat treatments performed. It shows a good strength while having an excellent elongation.
- Among the precipitation hardening processes proposed, the one which gives the best compromise of strength and elongation is the artificial ageing at 120ºC for 20 hours.
- In order to understand which precipitates are present inside the microstructure, a TEM analysis would be necessary.

The other two typologies of tensile test were interesting for understanding some properties related to the formability at high temperature of the material. The tests at room temperature, after the alloy was heated up to 3 different temperatures for 5 minutes, were useful to assess the properties of the material after stamping and to have an idea about the optimum warm forming temperature for the alloy. The three temperatures selected for the heating that precedes the tests at room temperature were 170, 200 and 230ºC. These values were chosen because, according to the information found in literature, they are close to the optimum warm forming temperature for a 7xxx series aluminum alloy. It must be kept in mind that 30 minutes have to be waited before carrying out the tensile test in order for the material to have time for cooling down completely at room temperature.

The tensile tests at high temperature, instead, were carried out in order to understand the elongation and maximum stress that the alloy shows at warm forming temperature. Thanks to this information, simulations of formability at high temperature could be performed. The temperature selected for the tests was 170ºC. Some considerations can be drawn from the results:

- Increasing the temperature of the heating performed before the tensile tests at room temperature, the mechanical properties of the alloy worsen as it was expected. At 170ºC we still have a good behavior, especially for what concerns the alloy aged at 120ºC for 20 hours (Figure 5.11), which also demonstrated to have a good elongation.
- Moreover, for what concerns the tests at room temperature with a previous heating of the material, the artificial ageing at 185ºC for 10 hours gives results not so satisfactory from the point of view of the elongation and it does not work harden properly. The ageing at 155ºC for 17 hours, instead, is a middle way between the other 2.
- During the tensile tests performed at 170ºC with the tensile machine connected to the environmental chamber (Figure 5.15), the UTS and the yield strength decreases consistently while the elongation increases a lot. The ductile behavior of the alloy is accentuated. The best compromise of strength and elongation is given by the material treated at 120ºC for 20 hours.

The last step of the experimental work was to perform a microstructural analysis of the fracture surfaces with the SEM on the fractured specimens after the tensile tests at room temperature. From the images taken, the fracture appeared as ductile with the presence of dimples for most of the conditions. The alloy aged at 155ºC for 17 hours and the one in the as received condition showed a brittle behavior. An inclusion was found in the fracture surface of the specimen aged at 120ºC for 20 hours. An EDS analysis was performed, which revealed the presence of iron. As seen in the literature review, an inclusion can be the cause of a crack initiation.

6. Conclusions

This thesis investigated basically two aspects of the aluminum alloy 7046. The first one was related to the definition of the heat treatment procedure which gives the best results in terms of mechanical properties. The second aspect concerned the study of the tensile properties of the material at room temperature, at warm forming temperature and after the alloy was heated up to a certain temperature for 5 minutes. The tensile properties were investigated both for the alloy in the as received condition and for the same alloy age hardened with the conditions established in the first part of the work. A microstructural analysis of the fracture surfaces was eventually conducted in order to discover the nature of the fracture.

- The solutionizing process selected is at 480ºC for 2 hours, followed by a quenching in icy water.
- The alloy aged at 120ºC for 20 hours gives the optimum mechanical properties in terms of elongation and strength.
- The tensile behavior of the material after it was heated to 170ºC for 5 minutes was still good enough, meaning that it could be a good temperature for warm forming.
- It was verified with the tests at high temperature that, again, the best compromise of strength and elongation was given by the ageing at 120ºC for 20 hours.
- The typology of fracture observed with the microstructural observation is ductile with the presence of dimples in most of the samples analyzed, excluding the alloy in the as received condition and the alloy aged at 155ºC for 17 hours.

6.1. Recommendations

For what concerns the possible future work on this project, some recommendations can be done:

- The data coming from the tensile tests performed at high temperature could be used, combined with the forming limit curves, for simulations of the behavior of the alloy in warm forming conditions.
- With some changes on the tensile machine that operates with the environmental chamber, other temperatures could be tried for the tensile tests.
- Different solution heat treatments could be tried in order to reduce even more the presence of impurities in the aluminum matrix.
- A combination of cold working and precipitation hardening could be performed on the alloy in order to verify if the strengthening effect changes.

References

[1] S. W. Hadley, S. Das and J. W. Miller, "Aluminum R&D for automotive uses and the department of energy's role," *Office of advanced automotive technologies - US department of energy,* vol. 1, pp. 1-28, 2000.

[2] Vox, "What are US fuel-efficiency standards for cars and trucks?," *[Online] Available: http://www.vox.com/cards/obama-climate-plan/what-are-u-s-fuel-efficiency-standards-for-cars-and-trucks [Accessed June 13th 2015]*.

[3] S. Glinton, "[Online] http://www.npr.org/2011/11/21/142464818/can-electric-cars-help-automakers-reach-55-mpg [Accessed June 25th 2015]," *White House fuel economy report, NHTSA,* 2011.

[4] M. Johannaber, M. Espig, R. Wohlecker, H. Wallentowitz and J. Leyers, "Determination of weight elasticity of fuel economy for conventional ICE vehicles, hybrid vehicles and fuel cell vehicles," *SAE technical paper,* pp. 1-7, 2007.

[5] D. V. Nieuwerburgh, "High ductile 6xxx and high strength 7xxx aluminum sheets for advanced "BIW" lightweight design," *AluMag Roadshow,* pp. 1-31, 2012.

[6] "Aluminum alloy families: strength metallurgy," *[Online] Available: http://www.imetllc.com/aluminum-alloy-families-strength-metallurgy/. [Accessed December 9th 2014]*.

[7] "Extrusion applications. Transportation - Auto," *[Online] Available: http://www.aec.org/extrusionapplications/auto.cfm [Accessed December 12th 2014]*.

[8] M. Tingting and A. Taylan, "Aluminum sheet forming for automotive applications, Part I: material properties and design guidelines," *Stamping Journal,* pp. 12-13, 2013.

[9] J. Zhang, Y. Deng, W. Yang, S. Hu and X. Zhang, "Design of the multi-stage quenching process for 7050 aluminum alloy," *Materials and Design,* vol. 56, pp. 334-344, 2013.

[10] S. Liu, Q. Zhong, Y. Zhang, W. Liu, X. Zhang and Y. Deng, "Investigation of quench sensitivity of high strength Al-Zn-Mg-Cu alloys by time-temperature-

properties diagrams," *Materials and Design,* vol. 31, pp. 3116-3120, 2010.

[11] M. Gwozdz and K. Kwapisz, "Influence of ageing process on the microstructure and mechanical properties of aluminum-silicon cast alloys - Al-9% Si-3% and Al-9% Si-0.4% Mg," *Bachelor degree thesis - Jonkoping University*, 2008.

[12] M. F. Ashby and R. H. Jones, Engineering Materials 2 - An introduction to microstructures, processing and design, Cambridge: Pergamon, 1986.

[13] E. Sjolander and S. Seifeddine, "The heat treatment of Al-Si-Cu-Mg casting alloys," *Journal of Materials Processing Technology*, vol. 210, pp. 1249-1259, 2010.

[14] "[Online] http://www.spaceflight.esa.int/, "European Space Agency"," [Accessed March 27th 2015].

[15] "7xxx-high strength aluminum sheets for lightweight automotive applications," *[Online] Alu-Report 03.2012 Automotive. Available: https://www.amag.at/fileadmin/user_upload/amag/Downloads/AluReport/EN/AR-2012-3-EN-AluReport_3_12_EN_S6-9.pdf*, [Accessed May 8th 2015].

[16] A. Mohamed and F. Samuel, "A review on the heat treatment of Al-Si-Cu/Mg casting alloys," *Metallurgy - Advances in Materials and Processes*, vol. InTech, pp. 58-69, 2012.

[17] N. Han, X. Zhang, S. Liu, D. He and R. Zhang, "Effect of solution treatment on the strength and fracture toughness of aluminum alloy 7050," *Journal of Alloys and Compounds*, vol. 509, pp. 4138-4145, 2011.

[18] K. Chen, H. Liu, Z. Zhang, S. Li and R. Todd, "The improvement of constituents dissolution and mechanical properties of 7055 aluminum alloy by stepped heat treatments," *Journal of Materials Processing Technology*, vol. 142, pp. 190-196, 2003.

[19] A. Mohamed, F. Samuel and S. Al Kahtani, "Influence of Mg and solution heat treatment on the occurrence of incipient melting in Al-Si-Cu-Mg cast alloys," *Materials Science and Engineering,* vol. 543, pp. 22-34, 2012.

[20] A. Samuel, H. Doty, S. Valtierra and F. Samuel, "Defects related to incipient melting in Al-Si-Cu-Mg alloys," *Materials and Design,* vol. 52, pp. 947-956, 2013.

[21] J. Sokolowski, X. C. Sun, G. Byczynski, D. Northwood, D. Penrod, R. Thomas and A. Esseline, "The removal of copper-phase segregation and the subsequent

improvement in mechanical properties of cast 319 aluminum alloys by a two-stage solution heat treatment," *Journal of Materials Processing Technology,* vol. 53, pp. 385-392, 1995.

[22] J. Sokolowski, M. B. Djurdjevic, C. A. Kierkus and D. O. Northwood, "Improvement of 319 aluminum alloy casting durability by high temperature solution treatment," *Journal of Materials Processing Technology ,* vol. 109, pp. 174-180, 2001.

[23] P. Li, B. Xiong, Y. Zhang and Z. Li, "Temperature variation and solution treatment of high strength AA 7050," *Trans. Nonferrous Met. Soc. China,* vol. 22, pp. 546-554, 2012.

[24] J. Samei and D. Green, "Lecture slides from "Characterization Techniques in Metal Forming"," *University of Windsor,* 2013.

[25] D. Hall and I. Mudawar, "Optimization of quench history of aluminum parts for superior mechanical properties," *International Journal Heat Mass Transfer,* vol. 39, pp. 81-95, 1996.

[26] J. F. Chinella and Z. Guo, "Computational thermodynamics characterization of 7075, 7039, and 7020 aluminum alloys using JMatPro," *Army Research Laboratory,* 2011.

[27] G. Sha and A. Cerezo, "Early-stage precipitation in Al-Zn-Mg-Cu alloy (7050)," *Acta Materialia,* vol. 52, pp. 4503-4516, 2004.

[28] Y. Liu, D. Jiang, B. Li, W. Yang and J. Hu, "Effect of cooling aging on microstructure and mechanical properties of an Al-Zn-Mg-Cu alloy," *Materials and Design,* vol. 57, pp. 79-86, 2014.

[29] P. Archambault and D. Godard, "High temperature precipitation kinetics and TTT curve of a 7xxx alloy by in-situ electrical resistivity measurements and differential calorimetry," *Scripta Materialia,* vol. 42, pp. 675-680, 2000.

[30] J. Buha, R. Lumley and A. Crosky, "Secondary ageing in aluminum alloy 7050," *Materials Science and Engineering,* vol. 492, pp. 1-10, 2008.

[31] W. D. Callister, Materials Science and Engineering: an introduction, John Wiley & Sons, 2007.

[32] J. Manickaraj, G. Liu and S. Shankar, "Effect of incubation coupled with artificial

aging in T6 heat treatment of A356.2 aluminum casting alloy," *International Journal of Metalcasting,* pp. 17-36, 2011.

[33] J. Tang, H. Chen, X. Zhang, W. Liu, H. Ouyang and H. Li, "Influence of quench-induced precipitation on aging behavior of Al-Zn-Mg-Cu alloys," *Trans. Nonferrous Met. Soc. China,* vol. 22, pp. 1255-1263, 2012.

[34] S. Liu, X. Zhang, M. Chen and J. You, "Influence of aging on quench sensitivity effect of 7055 aluminum alloy," *Materials Characterization,* vol. 59, pp. 53-60, 2008.

[35] L. Berg, J. Gjonnes, V. Hansen, X. Li, M. Knutson-Wedel, G. Waterloo, D. Schryvers and L. Wallenberg, "GP-zones in an Al-Zn-Mg alloy and their role in artificial aging," *Acta Materialia,* vol. 49, pp. 3443-3451, 2001.

[36] L. Wu, M. Seyring, M. Rettenmayr and W. Wang, "Characterization of precipitate evolution in an artificially aged Al-Zn-Mg-Sc-Zr alloy," *Materials Science and Engineering,* vol. A, pp. 1068-1073, 2010.

[37] M. Chemingui, M. Khitouni, G. Mesmacque and A. W. Kolsi, "Effect of heat treatment on plasticity of Al-Zn-Mg alloy: microstructure evolution and mechanical properties," *Elsevier Physics Procedia,* vol. 2, pp. 1167-1174, 2009.

[38] I. Sevim, S. Sahin, H. Cug, E. Cevik, F. Hayat and M. Karali, "Effect of aging treatment on surface roughness, mechanical properties, and fracture behavior of 6xxx and 7xxx aluminum alloys," *Strength of materials,* vol. 46, no. 2, pp. 190-197, 2014.

[39] R. A. Ayres, H. W. Lanning, B. Taylor and W. G. Heimburch, "Warm forming the GM V-6 oil pan in aluminum," *Society of Automotive Engineers,* pp. 1-5, 1978.

[40] L. R. Morris and R. A. George, "Warm forming high-strength aluminum automotive parts," *Society of Automotive Engineers,* pp. 1-9, 1977.

[41] B. Taylor, R. Heimbuch and S. G. Babcock, "Proceedings of the Second International Conference on Mechanical Behavior of Materials," *Federation of Materials Societies,* vol. 1, pp. 2004-2006, 1976.

[42] T. Mao and T. Altan, "Aluminum sheet forming for automotive applications, Part I," *Stamping Journal - FMA pubblication,* pp. 12-13, 2013.

[43] I. J. Polmear, Light alloys: metallurgy of the light metals, London: Edward Arnold,

1981.

[44] M. R. Clinch, R. Daval, S. J. Harris, W. Hepples, N. J. H. Holroyd, M. J. Lawday and B. Noble, "A microstructural engineering-based approach to 7xxx series alloy optimisation," *Materials forum,* vol. 28, pp. 145-151, 2004.

[45] S. K. Maloney, K. Hono, I. J. Polmear and S. P. Ringer, "The chemistry of precipitates in an aged Al-2.1Zn-1.7Mg at% alloy," *Scripta Materalia,* vol. 41, pp. 1031-1038, 1999.

[46] T. Pardoen, D. Dumont, A. Deschamps, Y. Brechet and J. Mech, "Grain boundary versus transgranular ductile fracture," *Journal of the Mechanics and Physics of Solids,* vol. 51, pp. 637-665, 2003.

[47] A. K. Mukhopadhyay, "Microstructure and properties of high strength aluminum alloys for structural applications," *Transactions of the Indian Institute of Metals,* vol. 62, no. 2, pp. 113-122, 2009.

[48] I. J. Polmear and M. J. Couper, "Design and development of an external wrought aluminum alloy for use at elevated temperatures," *Metallurgical transactions A,* vol. 19A, pp. 1027-1034, 1988.

[49] S. V. Senkova, R. B. Bhat and O. N. Senkov, "Microstructure and tensile properties of developmental Al-Zn-Mg-Cu cast alloys modified with Sc and Zr," *TMS Annual meeting,* 2005.

[50] O. N. Senkov, R. B. Bhat, S. V. Senkova and J. D. Schloz, "Microstructure and properties of cast ingots of Al-Zn-Mg-Cu cast alloys modified with Sc and Zr," *Metallurgical and materials transactions A,* vol. 36A, pp. 2115-2126, 2005.

[51] H. Zak and B. Tonn, "Effect of chemical composition on the microstructure, mechanical properties and susceptibility to hot tearing of high strength Al-Zn-Mg-Cu cast alloys," *EAA,* 2011.

[52] S. Bozorgi, M. Justl, L. Kniewallner and P. Schumacher, "Effect of alloying element (Magnesium, Zinc, Copper) on hot cracking susceptibility and mechanical properties of as-cast Al-Zn-Mg-Cu alloys," *EAA,* 2011.

[53] S. Hashemi, Foundations of materials science and engineering, McGraw-Hill, 2006.

[54] ASTM E8/E8M-15a, standard test methods for tension testing of metallic materials, page 3, ASTM International, 2015.

[55] G. Torres-Villasenor and E. Martinez-Flores, "Hybrid materials based on Zn-Al alloys," *Intech open science,* pp. 150-170, 2011.

[56] "Metallographic etchants - Aluminum," *[Online] Available: http://www.metallographic.com/Etchants/Aluminum%20etchants.htm [Accessed February 2nd 2015],* 2006.

[57] M. Gasko and G. Rosenberg, "Correlation between hardness and tensile properties in ultra-high strength dual phase steel-short communication," *Materials Engineering,* vol. 18, pp. 155-159, 2011.

[58] "Vickers indentation using CSM's Micro Scratch Test (MST)," *CSM instruments, [Online] Available: http://www.csm-instruments.com/Vickers-indentation-using-CSMs-Micro-Scratch-Tester. [Accessed June 14th 2015]*.

Vita Auctoris

NAME:	Sergio Barberis Pinlung
PLACE OF BIRTH:	Gattinara, Italy
YEAR OF BIRTH:	1991
EDUCATION:	Liceo Scientifico Tecnologico, Valle Mosso, Italy, 2010
	Politecnico di Torino, B.Sc. in Automotive Engineering, Torino, Italy, 2010-2013
	Politecnico di Torino, M.A.Sc. in Automotive Engineering, Torino, Italy, 2013-2015
	University of Windsor. International M.A.Sc. in Mechanical Engineering, Windsor, Canada, 2014-2015